

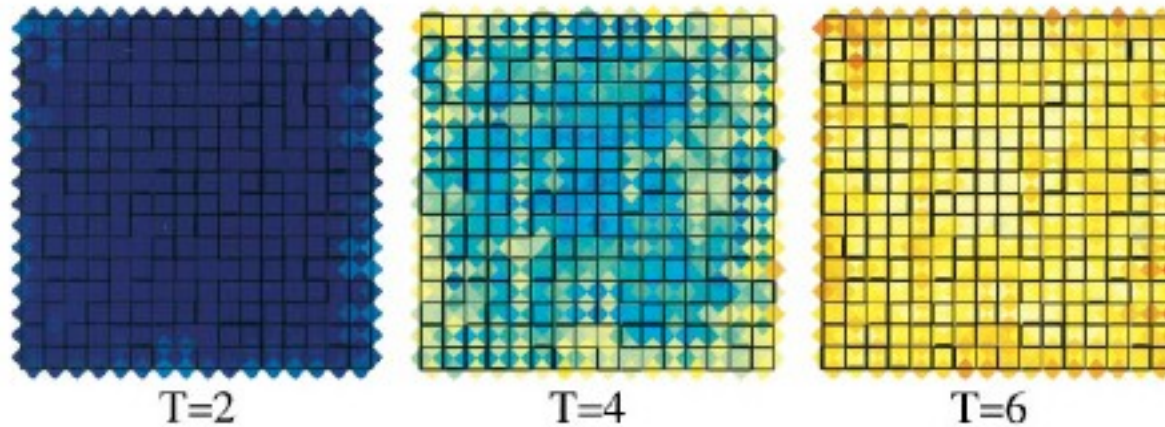
New Phase Transition Phenomena in Systems with Frozen Disorder

5 February 2009, University of Oldenburg

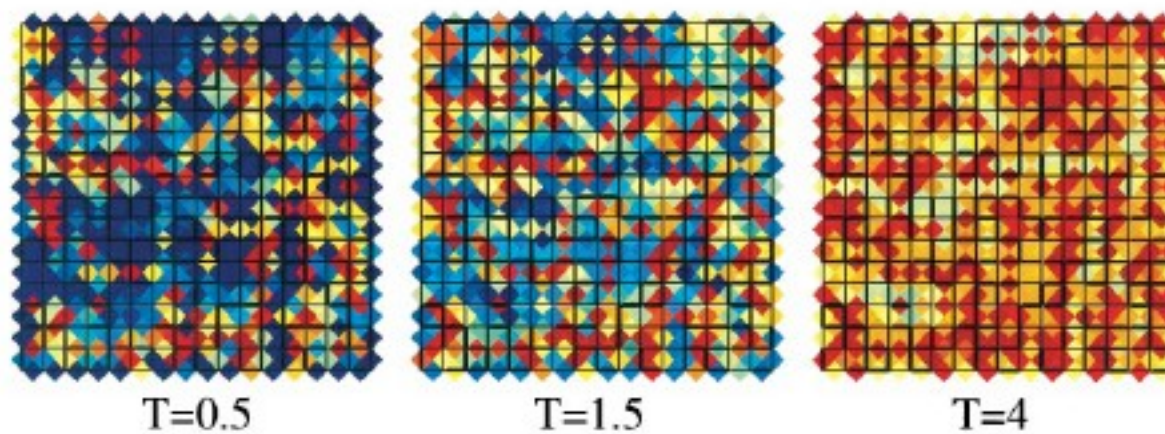


Istanbul, Turkey

Random Bond Correlations ($d=2$)



Spin-Glass Correlations ($d=2$)



$\langle s_i s_j \rangle$

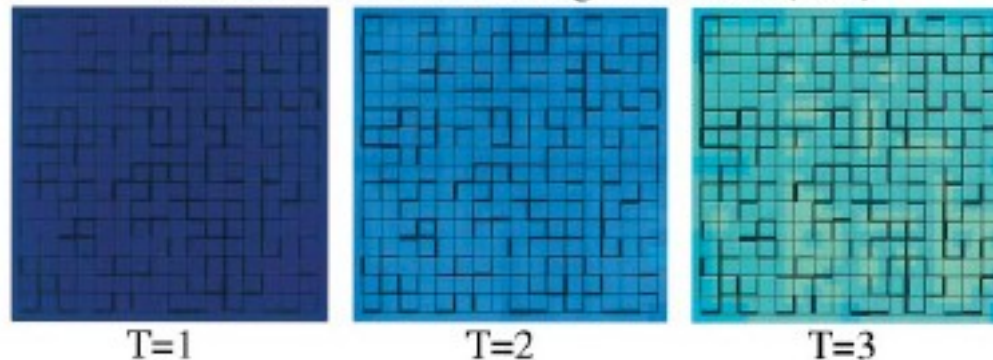
0

1

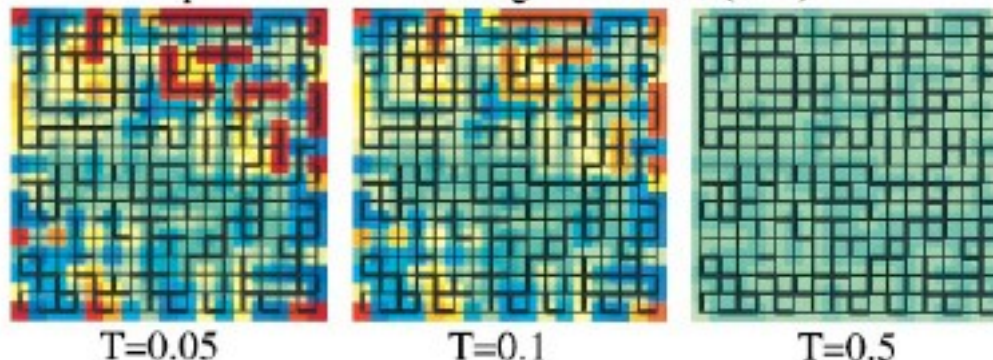
Equilibrium: Local renormalization-group theory

D. Yeşiltepen and ANB, 1997

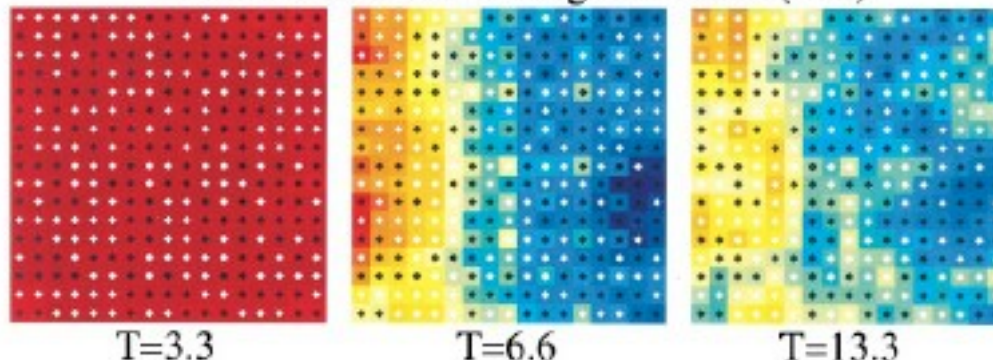
Random-Bond Local Magnetizations (d=2)



Spin-Glass Local Magnetizations (d=2)



Random-Field Local Magnetizations (d=3)

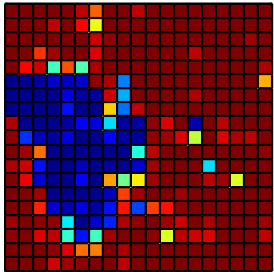


$\langle S_i \rangle$

-1

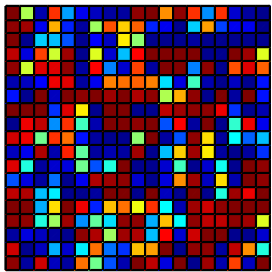
1

Local Magnetizations in the Ferromagnetic Hysteresis Loop



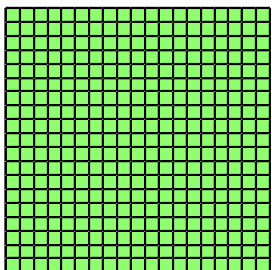
$H_Q = 0, M^{(0)} = 0.70 \quad H_Q = -0.595, M = 0 \quad H_Q = 0, M = -0.70$

Local Magnetizations in the Spin-Glass Hysteresis Loop



$H_Q = 0, Q^{(0)} = 0.68 \quad H_Q = -0.375, Q = 0 \quad H_Q = 0, Q = -0.68$

Local Magnetizations in the Paramagnetic Phase



$H_Q = 0, M^{(0)} = 0$



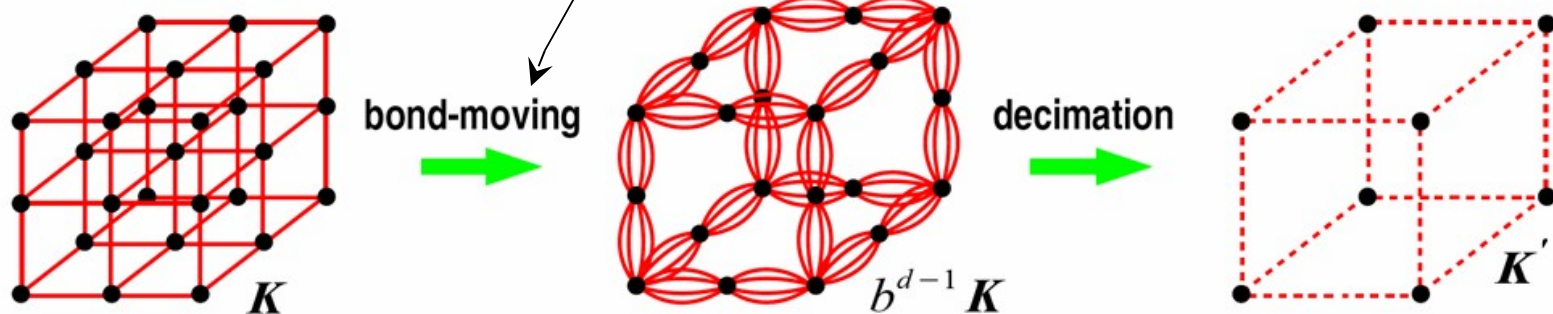
Non-equilibrium:
Local hard-spin mean-field theory
B. Yücesoy and ANB, 2007

Renormalization-Group Transformation for a Cubic Lattice ($d=3$)

(Approximate)

Migdal-Kadanoff procedure for d dimensional hypercubic lattice, with length rescaling factor b :

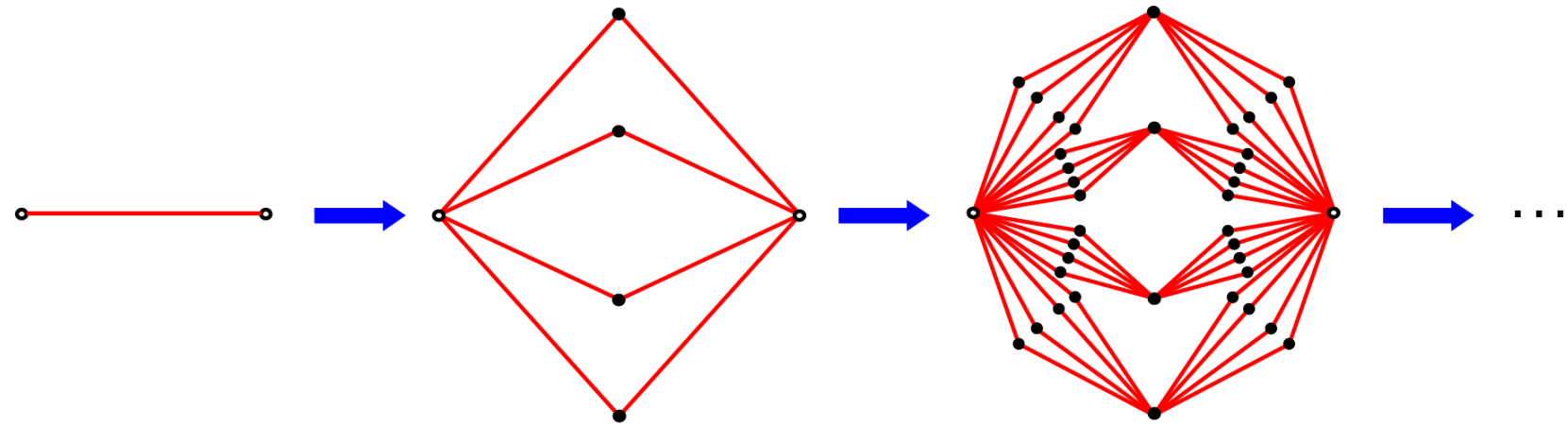
Example with $d = 3, b = 2$



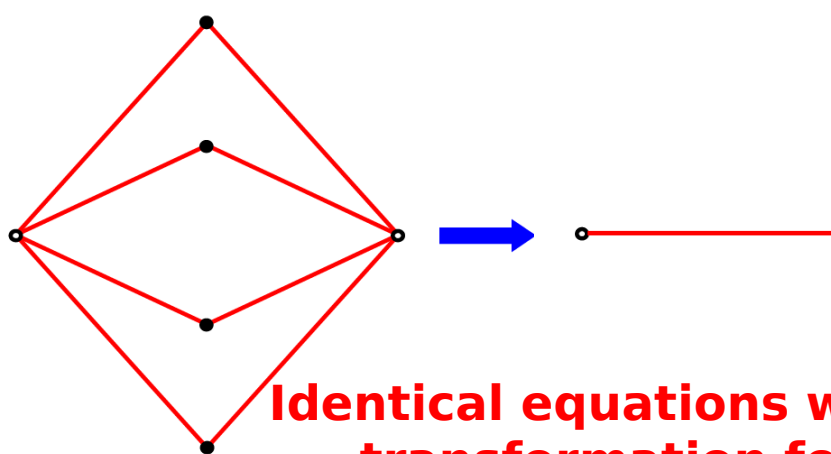
Construction of a Hierarchical Lattice ($d=3$)

Length rescaling factor, $b = 2$

Volume rescaling factor, $b^d = 8$



Renormalization-Group Transformation for this Hierarchical Lattice
(exact)

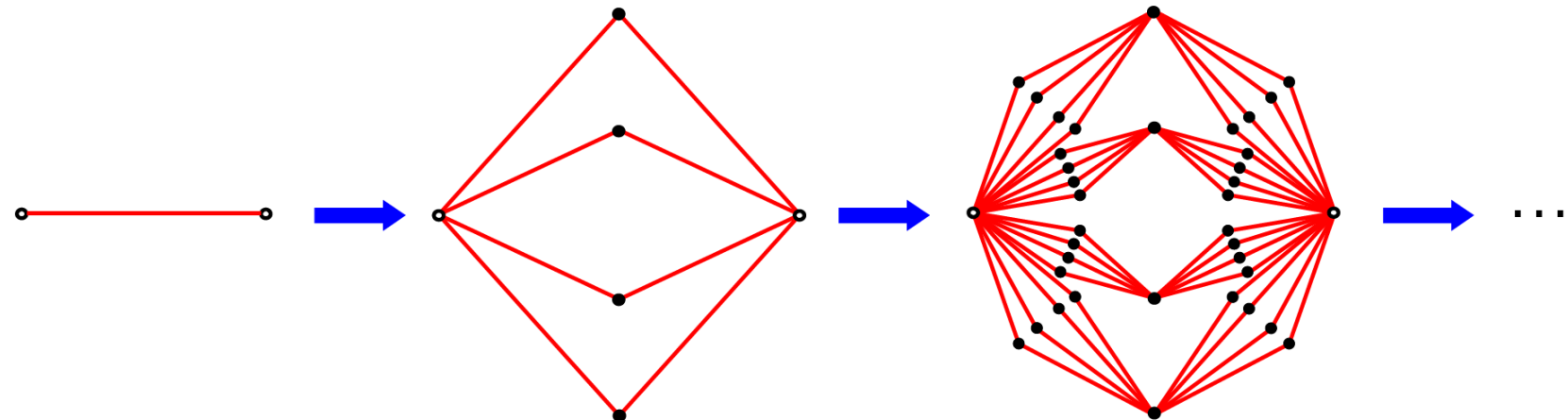


Identical equations with the approximate transformation for the cubic lattice

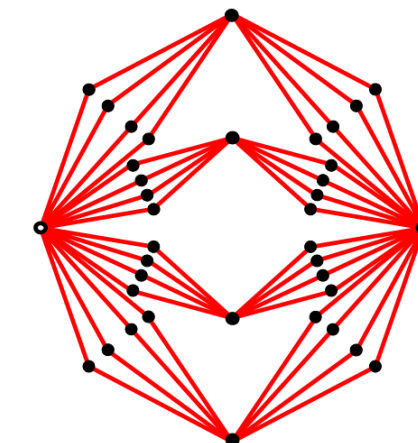
Construction of a Hierarchical Lattice ($d=3$)

Length rescaling factor, $b = 2$

Volume rescaling factor, $b^d = 8$



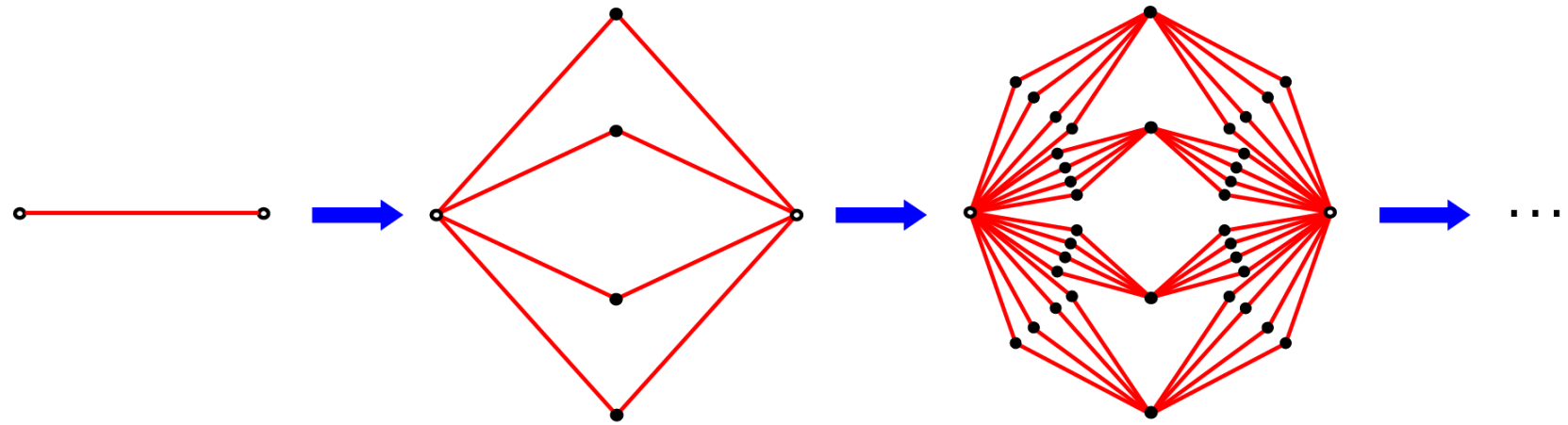
Renormalization-Group Transformation for this Hierarchical Lattice
(exact)



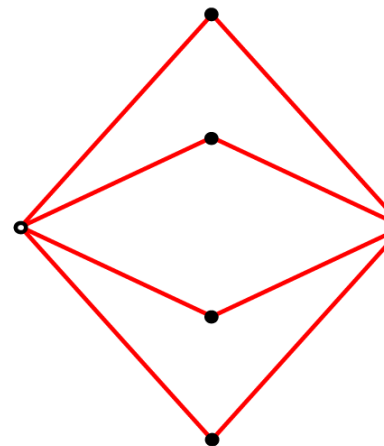
Construction of a Hierarchical Lattice ($d=3$)

Length rescaling factor, $b = 2$

Volume rescaling factor, $b^d = 8$



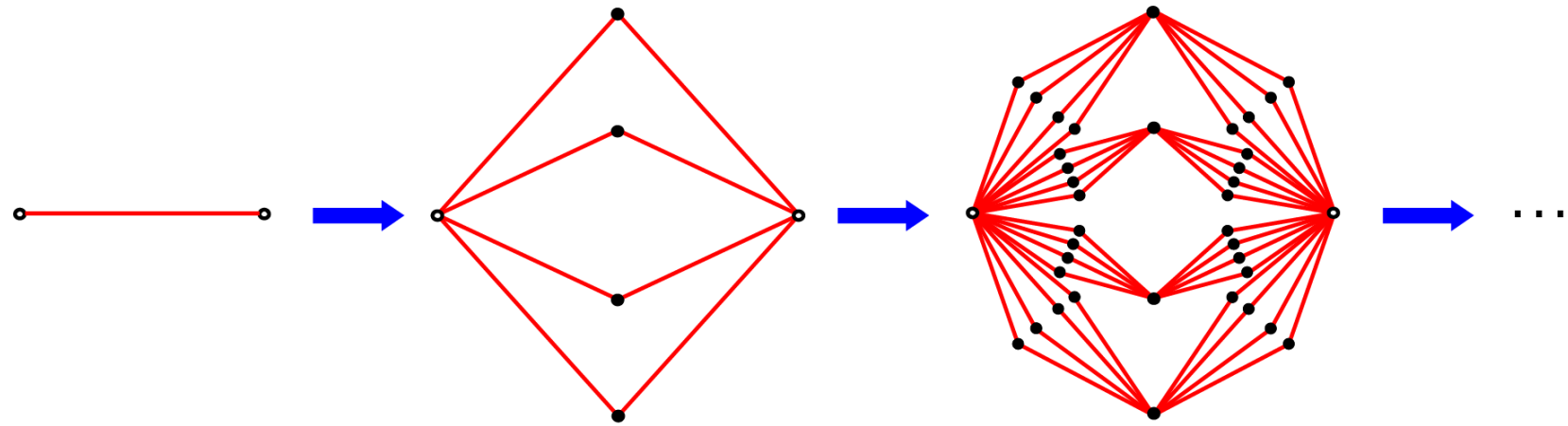
Renormalization-Group Transformation for this Hierarchical Lattice
(exact)



Construction of a Hierarchical Lattice ($d=3$)

Length rescaling factor, $b = 2$

Volume rescaling factor, $b^d = 8$



Renormalization-Group Transformation for this Hierarchical Lattice
(exact)



Hierarchical Lattices

Any imbedding graph or graphs can be used.

Any dimensionality, other effects (frustration) can be realized.

Exactly soluble by renormalization-group theory

Multicritical phenomena

Random-bond, random-field systems, spin glasses

Chaotic renormalization-group trajectories

Electronic models for high-T_c superconductivity

Scale-free networks with tunable clustering

...

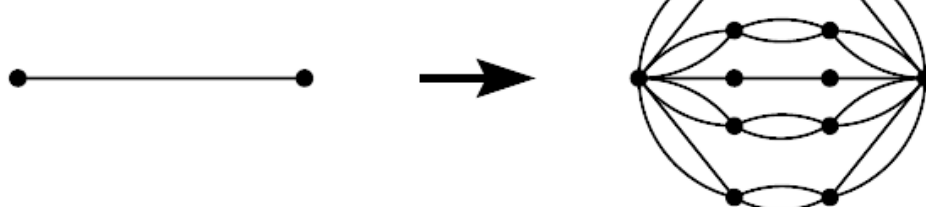
Lattice vibrations

Directed paths and polymers

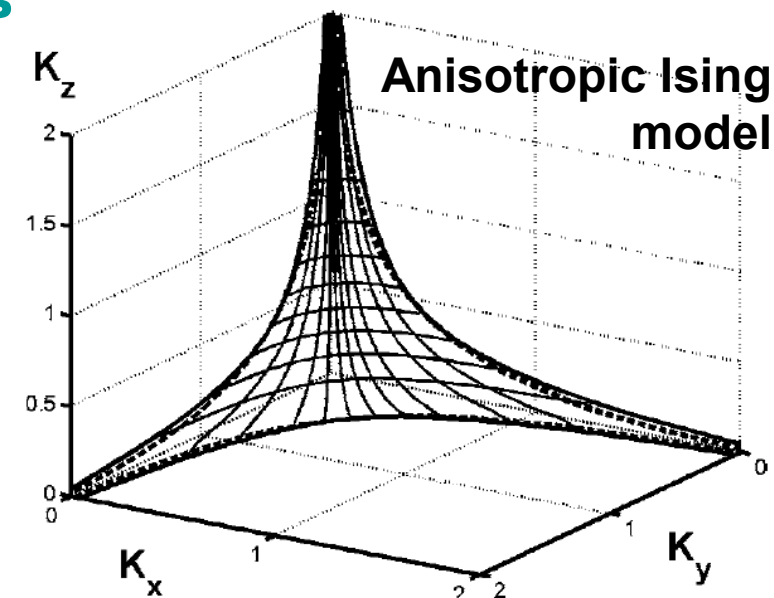
Schrödinger equation

...

In RG works below: $d = 3$



A. Erbaş, et al., Phys. Rev. E 72, 026129 (2005).



Systems with Quenched Random Interactions

Renormalization of the Quenched Probability Distribution

$$P'(\mathbf{K}'_{i'j'}) = \int \left(\prod_{ij}^{i'j'} d\mathbf{K}_{ij} P(\mathbf{K}_{ij}) \right) \delta(\mathbf{K}'_{i'j'} - \mathbf{R}(\{\mathbf{K}_{ij}\}))$$

local RG
recursion
relation

New Phase Transition Phenomena in Systems with Frozen Disorder

1. Inverted Tricritical Points of the BEG Spin-Glass in d=3

V.O. Özçelik and ANB, Phys. Rev. E 78, 031104 (2008).

2. Quenched Vacancy Induced Spin-Glass Phase and Temperature Reentrance in d=3

G. Gülpınar and ANB, [arXiv:0811.0025v1](#), Phys. Rev. E, in press (2009).

3. Quantum Spin-Glasses and Phase Diagram Asymmetry in d >2

C.N. Kaplan and ANB, Phys. Rev. Lett. 100, 027204 (2008).

4. Quenched Bond Randomness Induced Criticality and the Strong Violation of Universality

A. Malakis, ANB, I.A. Hadjiagapiou, N.G. Fytas, Phys. Rev. E 79, 011125 (2009)

5. Infinitely Robust Order and Local Order-Parameter Tulips in Apollonian Networks with Quenched Disorder

C.N. Kaplan, M. Hinczewski, and ANB, [arXiv:0811.3437v1](#) (2008).

I. Inverted Tricritical Points of the BEG Spin-Glass in d=3

V.O. Özçelik and ANB, Phys. Rev. E 78, 031104 (2008).

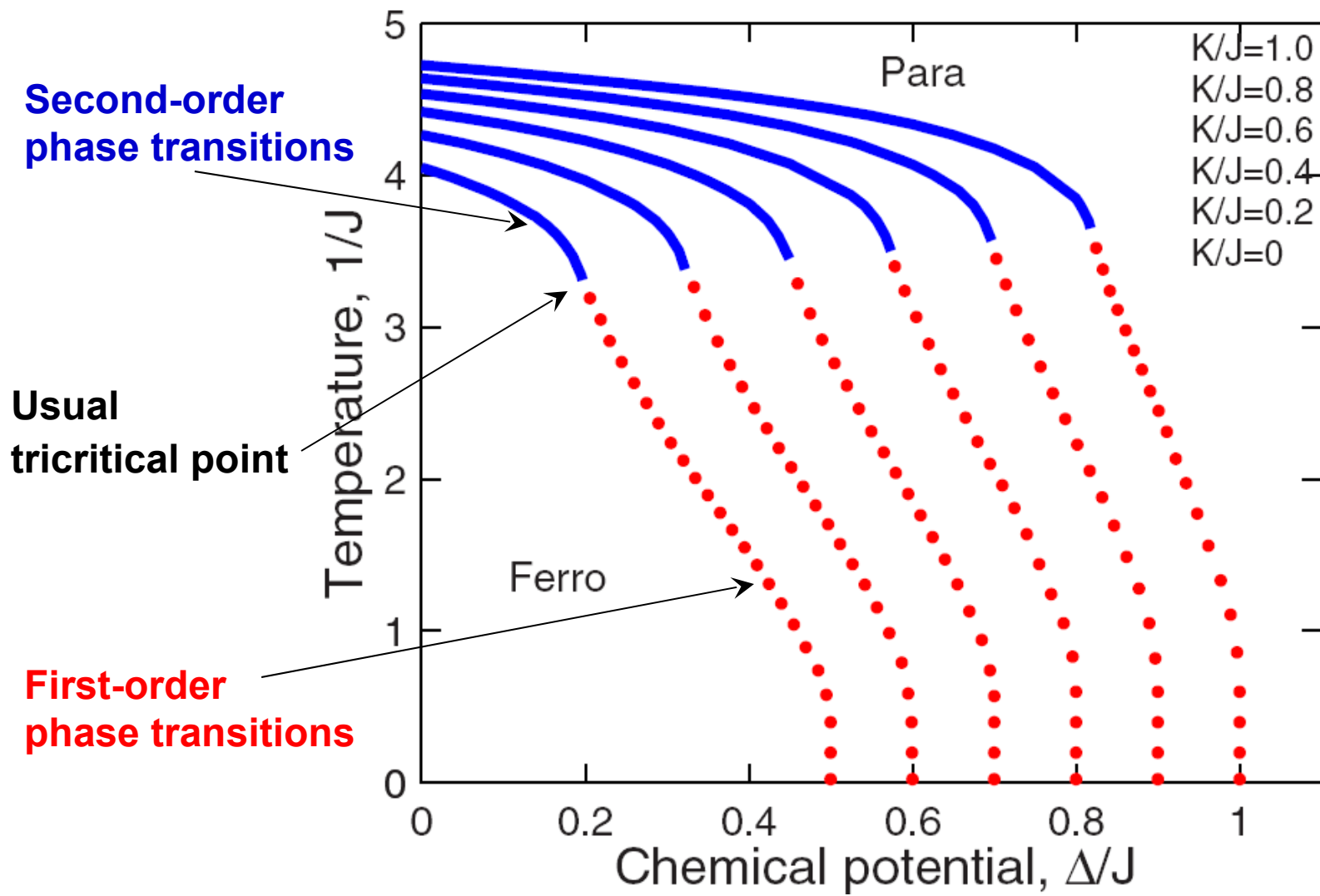
Blume-Emery-Griffiths Spin-Glass System

$$-\beta \mathcal{H} = \sum_{\langle ij \rangle} [J_{ij} s_i s_j + K s_i^2 s_j^2 - \Delta(s_i^2 + s_j^2)],$$

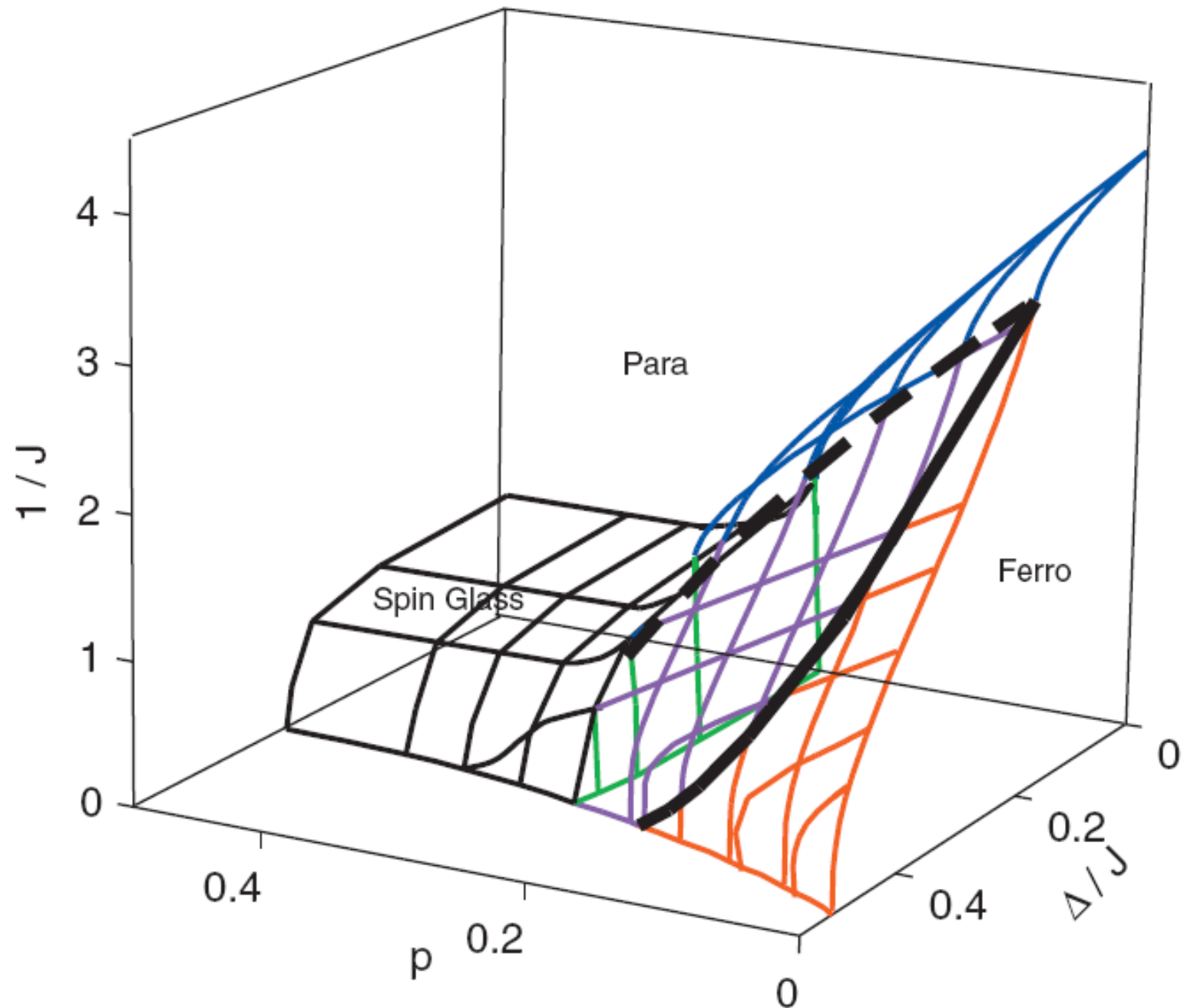
$$s_i = \pm 1, 0$$

$J_{ij} = + J$ (*ferromagnetic*) *with probability 1-p*

$J_{ij} = - J$ (*antiferromagnetic*) *with probability p*



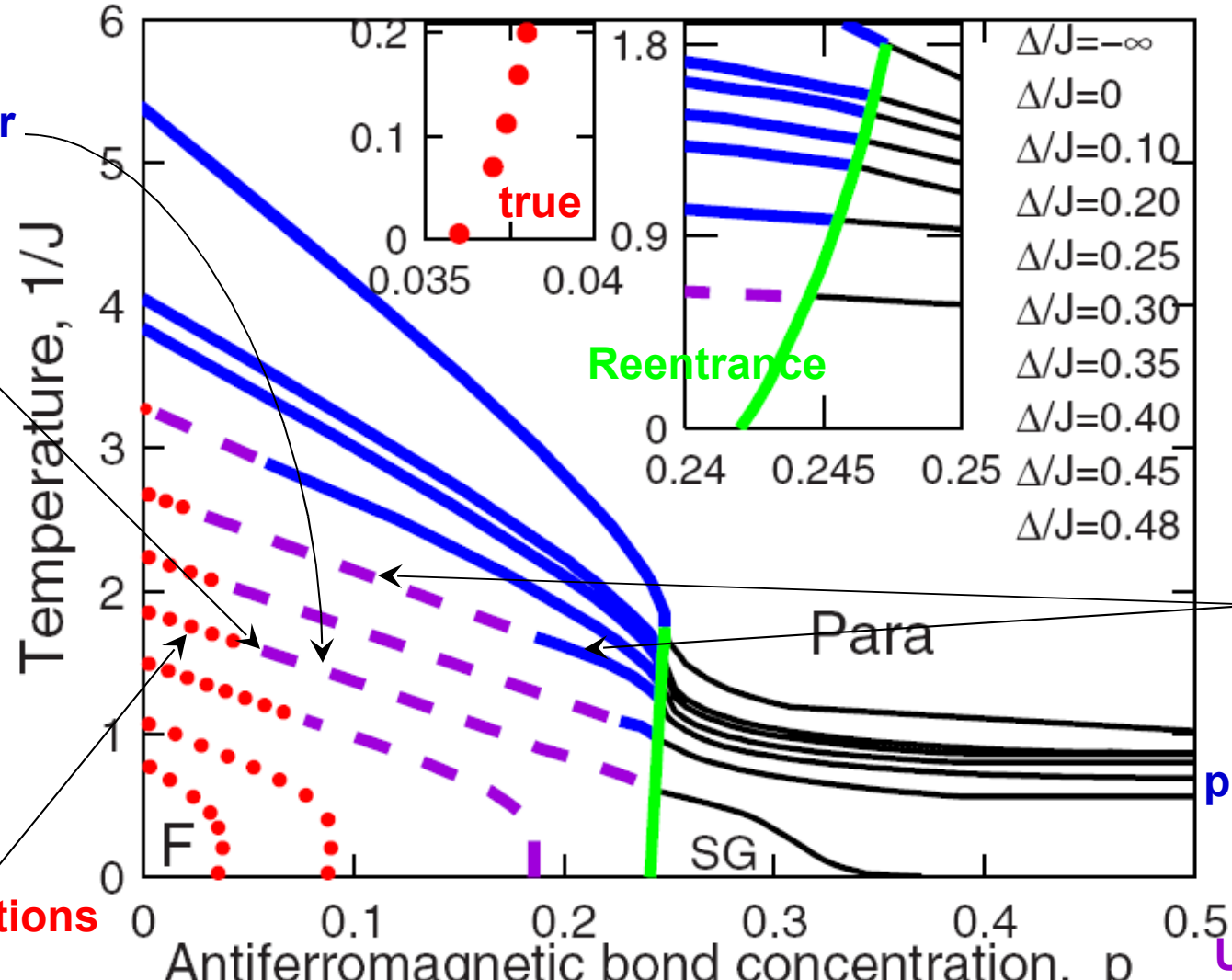
No antiferromagnetic bonds ($p=0$)



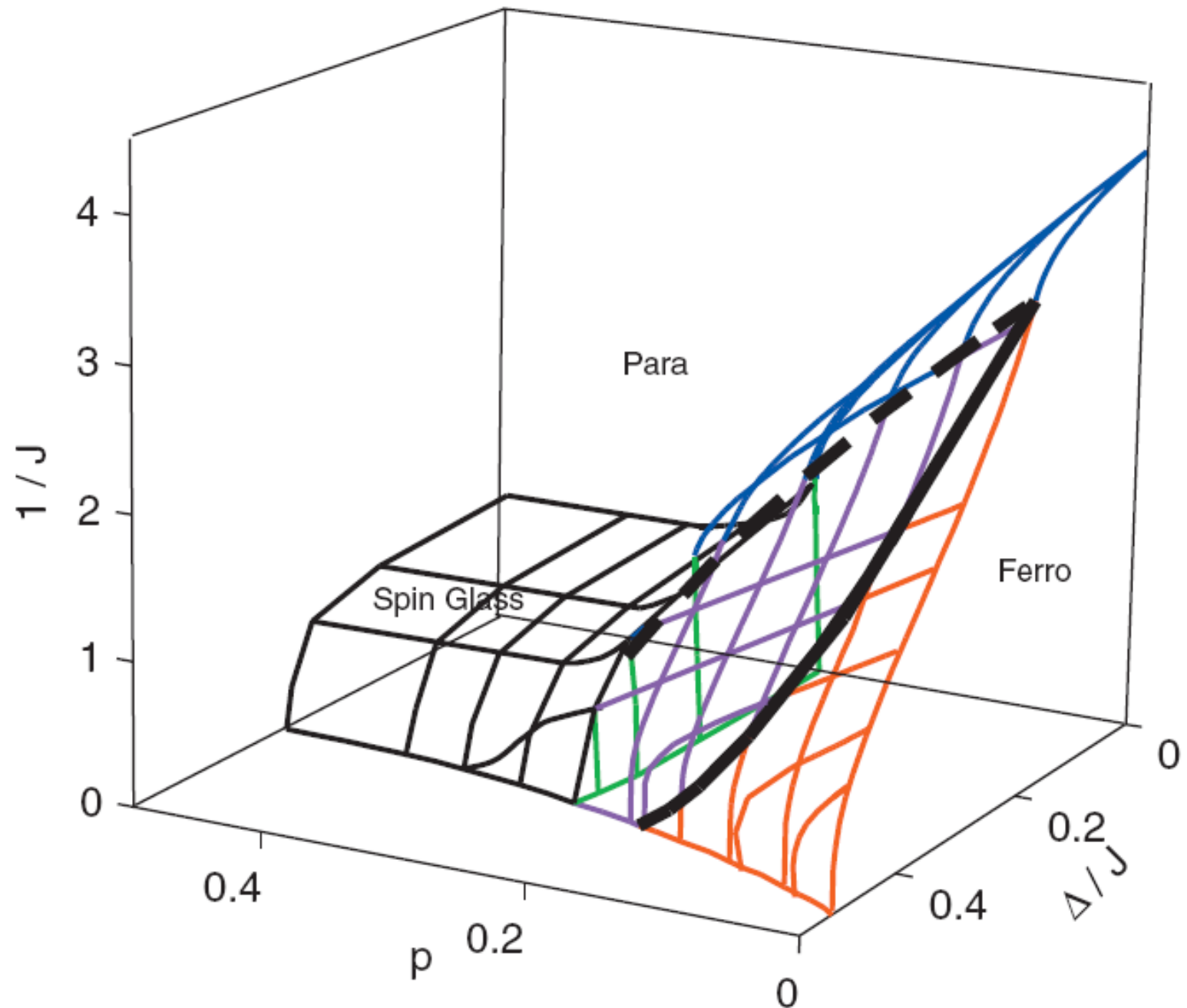
New
second-order
phase trans.

Inverted
tricritical
point

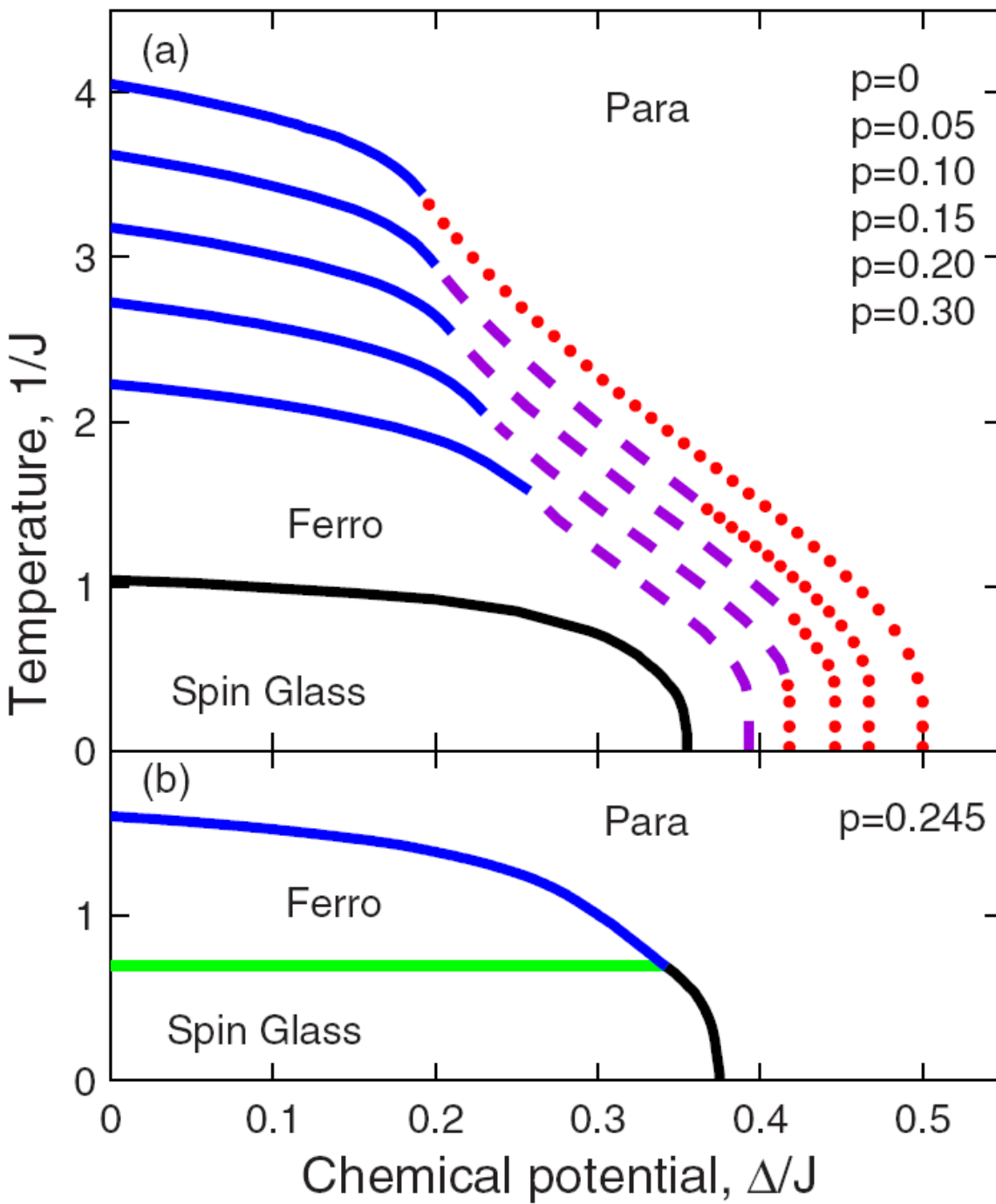
First-order
phase transitions



With antiferromagnetic bonds of concentration p

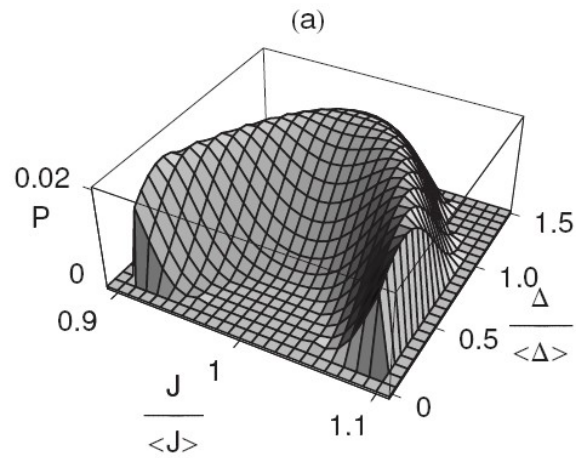


**Complete
reentrance**

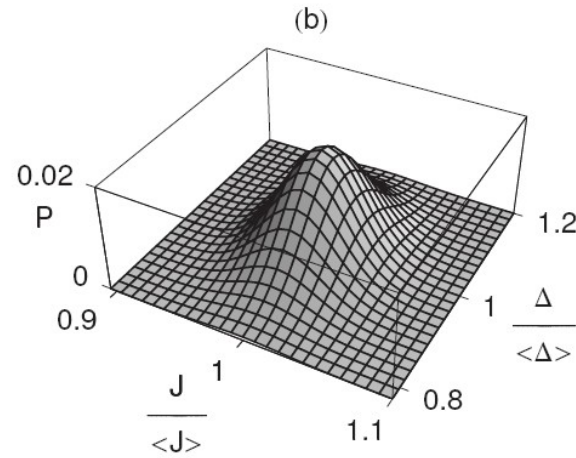


Renormalization-Group Fixed Distributions

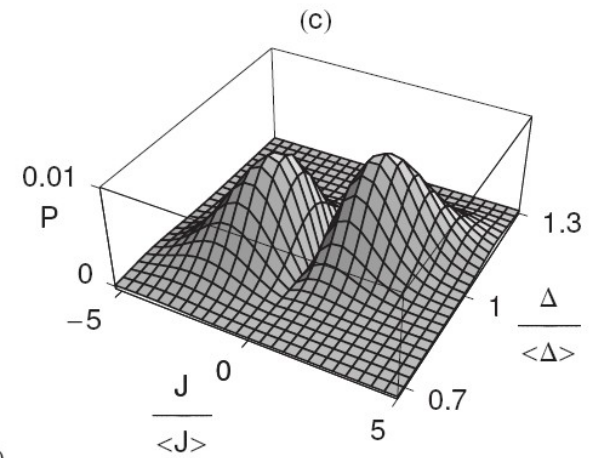
Ferro-Para
2nd order



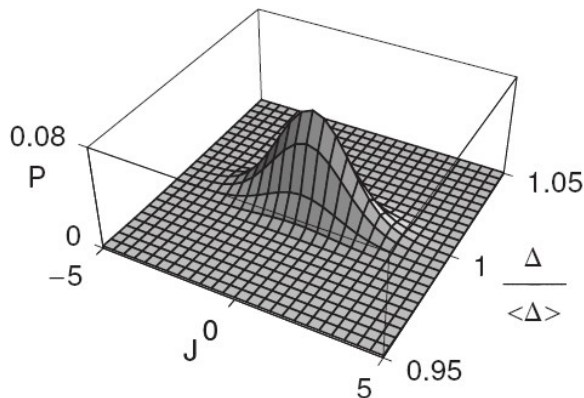
Ferro-Para
1st order



Ferro-SG
2nd order

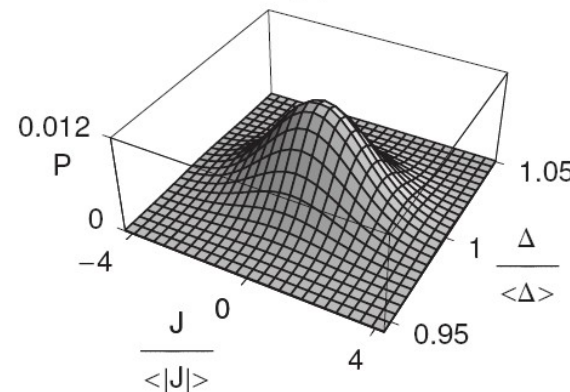


(d)



SG-Para
2nd order

(e)



SG sink

II. Quenched Vacancy Induced Spin-Glass Phase and Temperature Reentrance in d=3

G. Gülpınar and ANB, arXiv:0811.0025v1, Phys. Rev. E, in press (2009).

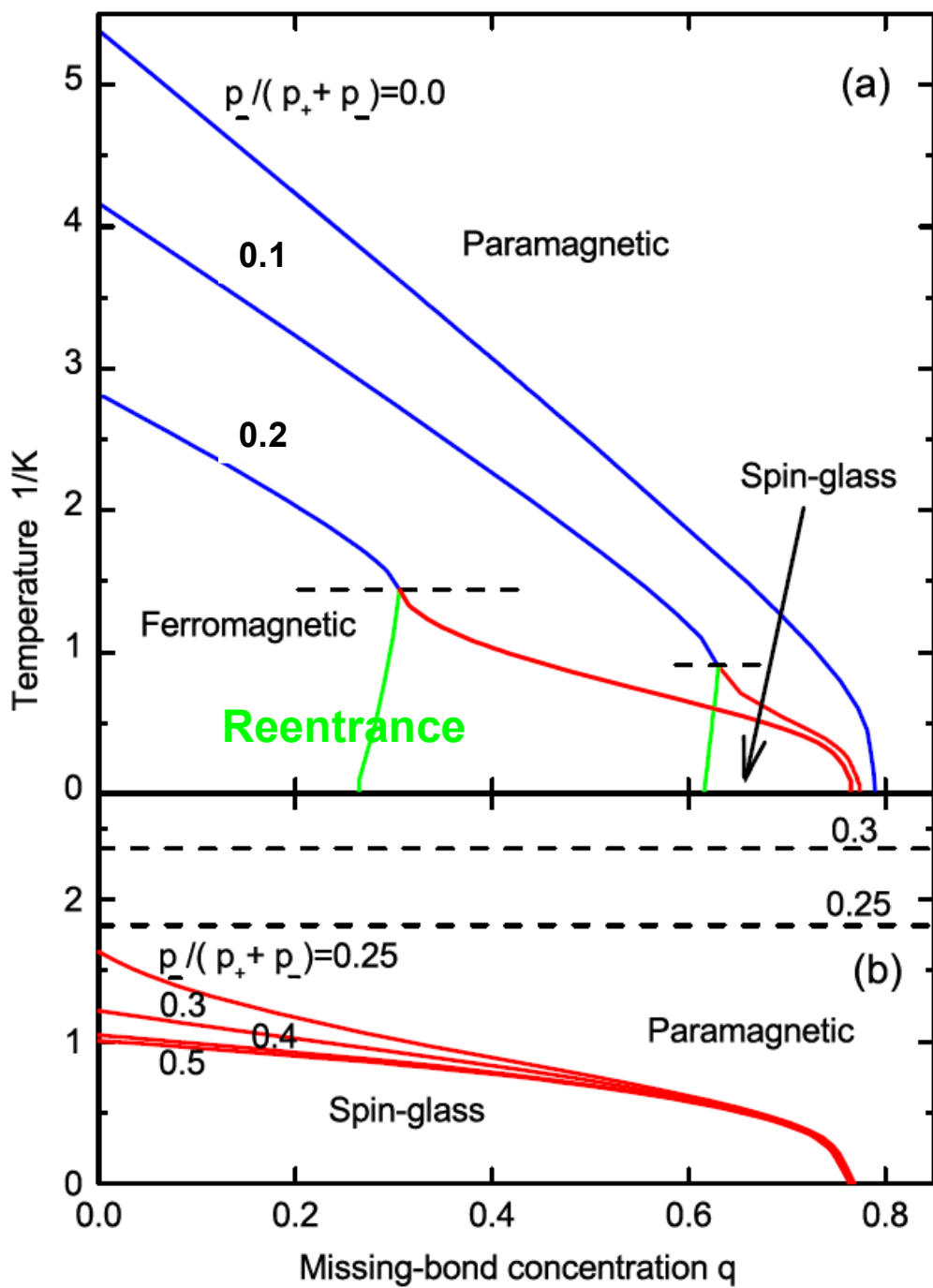
$$-\beta H = \sum_{\langle ij \rangle} K_{ij} s_i s_j ,$$

$$s_i = \pm 1$$

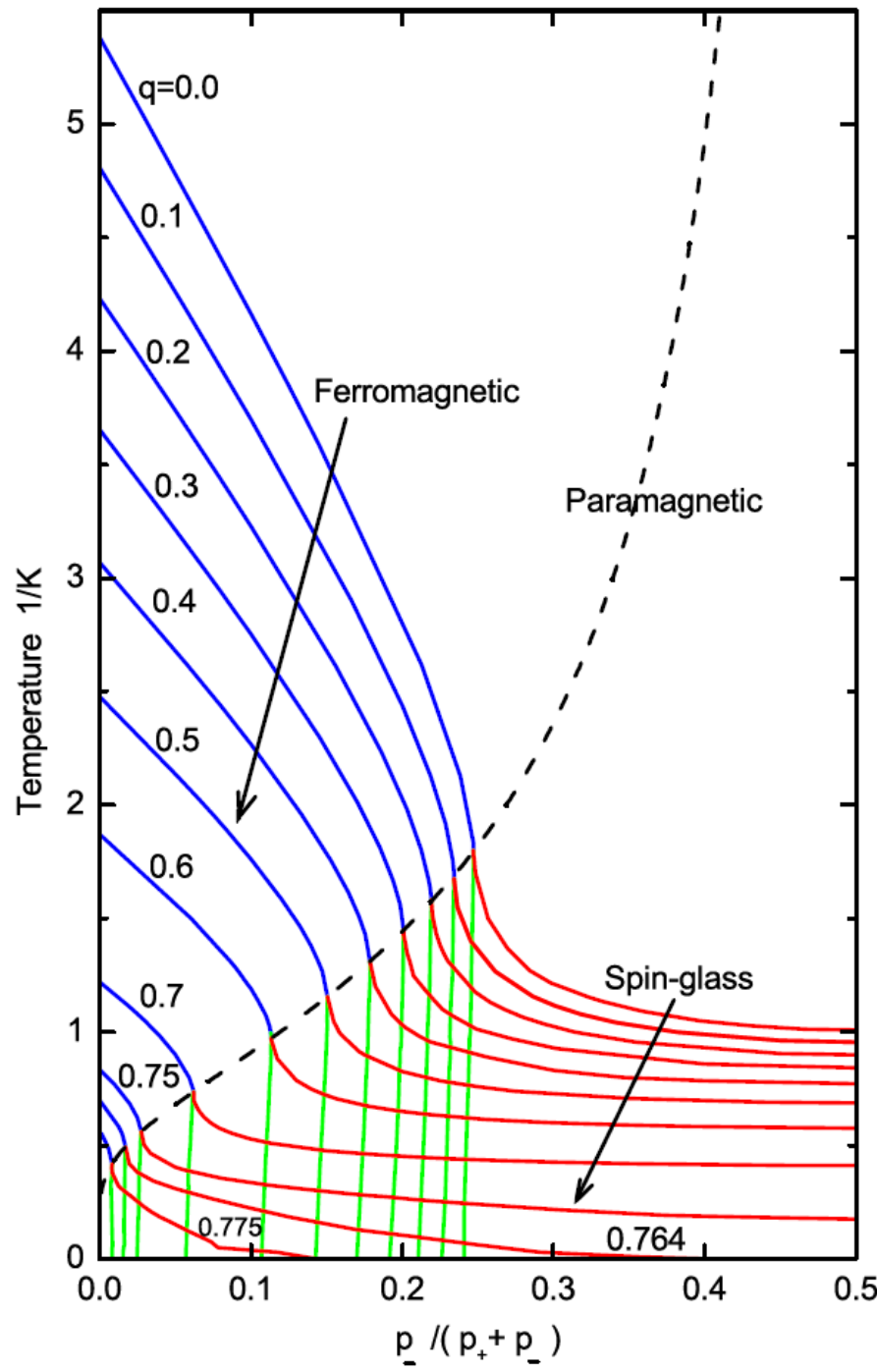
$K_{ij} = +K$ (*ferromagnetic*) *with probability p_+*

$K_{ij} = -K$ (*antiferromagnetic*) *with probability p_-*

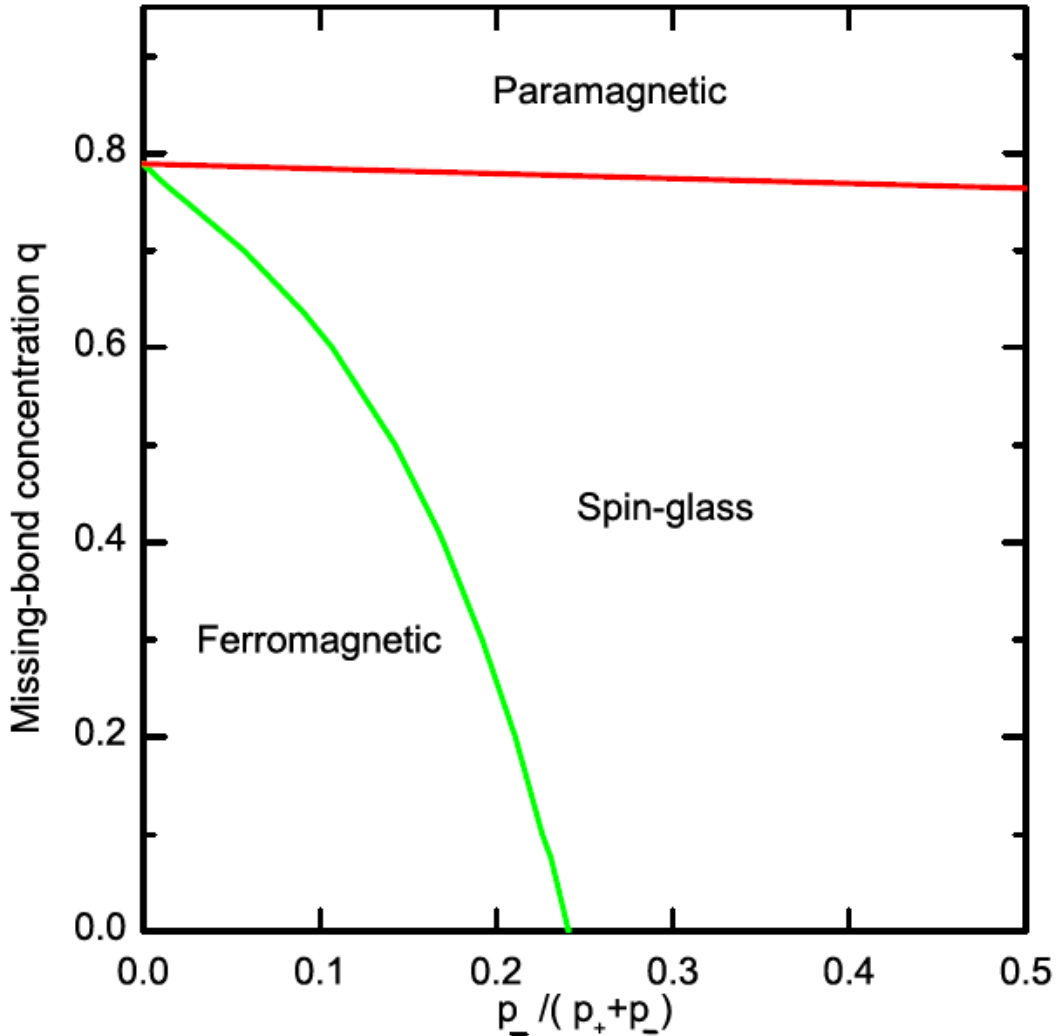
$K_{ij} = 0$ (*missing bond*) *with probability $q = 1 - p_+ - p_-$*



Reentrance



Zero-Temperature Phase Diagram



A. Aharony, J. Phys. C 11, L457 (1978).

B.W. Southern, A.P. Young, and P. Pfeuty, J. Phys. C 12, 683 (1979).

A. Aharony and K. Binder, J. Phys. C 13, 4091 (1980)

A.J. Bray and S. Feng, Phys. Rev. B 36, 8456 (1987).

III. Quantum Spin-Glasses and Phase Diagram Asymmetry in $d > 2$

C.N. Kaplan and ANB, Phys. Rev. Lett. 100, 027204 (2008).

$$-\beta \mathcal{H} = \sum_{\langle ij \rangle} J_{ij} \mathbf{s}_i \cdot \mathbf{s}_j$$

Heisenberg quantum spin operators s_i

$J_{ij} = +J$ (*ferromagnetic*) *with probability 1-p*

$J_{ij} = -J$ (*antiferromagnetic*) *with probability p*

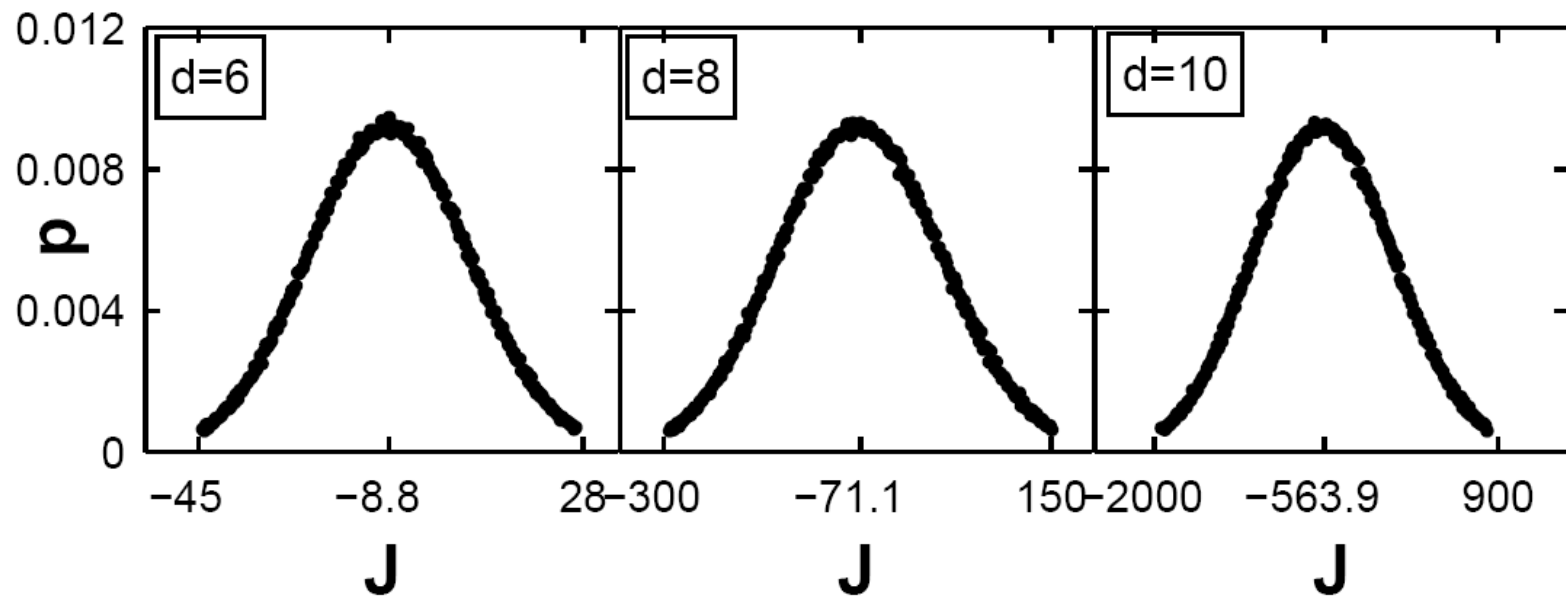
A quantum spin-glass system

Renormalization of the Frozen Probability Distribution

$$\mathcal{P}'(J'_{i'j'}) = \int \left[\prod_{ij}^{i'j'} dJ_{ij} \mathcal{P}(J_{ij}) \right] \delta(J'_{i'j'} - R(\{J_{ij}\}))$$

↑
from

Suzuki-Takano (quantum)
Migdal-Kadanoff ($d > 1$)



Unstable (critical) fixed distributions

$$\begin{aligned}
\text{Tr}_{(j,k)} e^{-\beta \mathcal{H}} &= \text{Tr}_{(j,k)} e^{\sum_i^{4n} \{-\beta \mathcal{H}(i,j) - \beta \mathcal{H}(j,k) - \beta \mathcal{H}(k,l)\}} \\
&\simeq \prod_i^{4n} \text{tr}_{(j,k)} e^{\{-\beta \mathcal{H}(i,j) - \beta \mathcal{H}(j,k) - \beta \mathcal{H}(k,l)\}} \\
&= \prod_i^{4n} e^{-\beta' \mathcal{H}'(i,l)} \simeq e^{\sum_i^{4n} \{-\beta' \mathcal{H}'(i,l)\}} \\
&= e^{-\beta' \mathcal{H}'},
\end{aligned}$$

M. Suzuki and H. Takano, 1979
H. Takano and M. Suzuki, 1981

$$\langle u_i z_l | e^{-\beta' \mathcal{H}'(i,l)} |\bar{u}_i \bar{z}_l \rangle =$$

$$\sum_{v_j,w_k} \langle u_i v_j w_k z_l | e^{-\beta \mathcal{H}(i,j) - \beta \mathcal{H}(j,k) - \beta \mathcal{H}(k,l)} |\bar{u}_i v_j w_k \bar{z}_l \rangle,$$

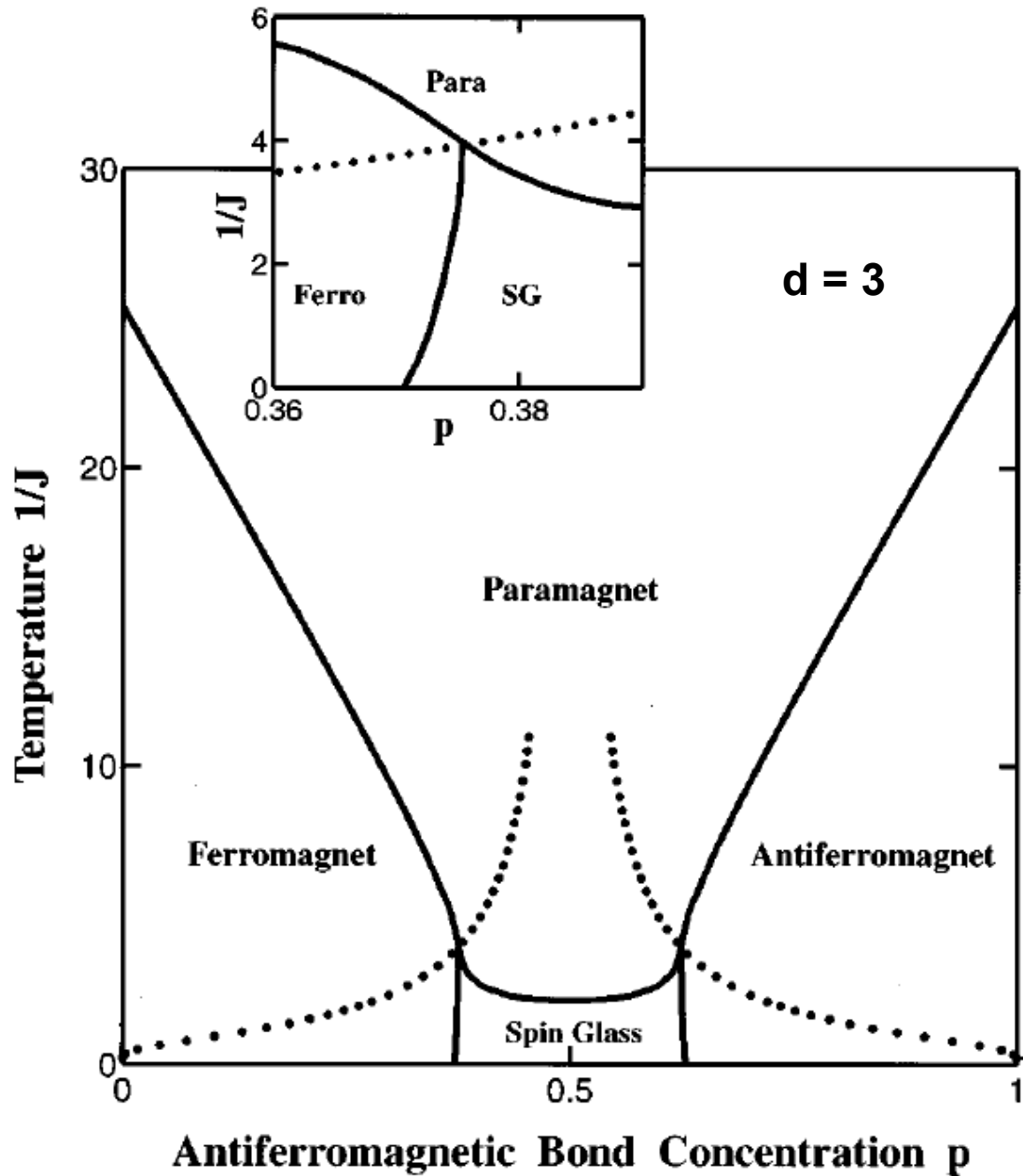
$$\begin{aligned} \langle \phi_p | e^{-\beta' \mathcal{H}'(i,l)} |\phi_{\bar{p}} \rangle &= \sum_{\substack{u,z,\bar{u}, \\ \bar{z},v,w}} \sum_{q,\bar{q}} \langle \phi_p | u_i z_l \rangle \langle u_i v_j w_k z_l | \psi_q \rangle \\ &\quad \times \langle \psi_q | e^{-\beta \mathcal{H}(ij) - \beta \mathcal{H}(j,k) - \beta \mathcal{H}(k,l)} | \psi_{\bar{q}} \rangle \\ &\quad \times \langle \psi_{\bar{q}} | \bar{u}_i v_j w_k \bar{z}_l \rangle \langle \bar{u}_i \bar{z}_l | \phi_{\bar{p}} \rangle. \end{aligned}$$

p	s	m_s	Two-Site Eigenstates
+	1	1	$ \phi_1\rangle = \uparrow\uparrow\rangle$
+	1	0	$ \phi_2\rangle = \frac{1}{\sqrt{2}}\{ \uparrow\downarrow\rangle + \downarrow\uparrow\rangle\}$
-	0	0	$ \phi_4\rangle = \frac{1}{\sqrt{2}}\{ \uparrow\downarrow\rangle - \downarrow\uparrow\rangle\}$

p	s	m_s	Four-Site Eigenstates
+	2	2	$ \psi_1\rangle = \uparrow\uparrow\uparrow\uparrow\rangle$
+	2	1	$ \psi_2\rangle = \frac{1}{2}\{ \uparrow\uparrow\uparrow\downarrow\rangle + \uparrow\uparrow\downarrow\uparrow\rangle + \uparrow\downarrow\uparrow\uparrow\rangle + \downarrow\uparrow\uparrow\uparrow\rangle\}$
+	2	0	$ \psi_3\rangle = \frac{1}{\sqrt{6}}\{ \uparrow\uparrow\downarrow\downarrow\rangle + \uparrow\downarrow\uparrow\downarrow\rangle + \uparrow\downarrow\downarrow\uparrow\rangle + \downarrow\uparrow\uparrow\downarrow\rangle + \downarrow\uparrow\downarrow\uparrow\rangle + \downarrow\downarrow\uparrow\uparrow\rangle\}$
+	1	1	$ \psi_6\rangle = \frac{1}{2}\{ \uparrow\uparrow\uparrow\downarrow\rangle - \uparrow\uparrow\downarrow\uparrow\rangle - \uparrow\downarrow\uparrow\uparrow\rangle + \downarrow\uparrow\uparrow\uparrow\rangle\}$
+	1	0	$ \psi_7\rangle = \frac{1}{\sqrt{2}}\{ \downarrow\uparrow\uparrow\downarrow\rangle - \uparrow\downarrow\uparrow\downarrow\rangle\}$
-	1	1	$ \psi_9\rangle = \frac{1}{2}\{ \uparrow\uparrow\uparrow\downarrow\rangle - \uparrow\uparrow\downarrow\uparrow\rangle + \uparrow\downarrow\uparrow\uparrow\rangle - \downarrow\uparrow\uparrow\uparrow\rangle\}, \psi_{10}\rangle = \frac{1}{2}\{ \uparrow\uparrow\uparrow\downarrow\rangle + \uparrow\uparrow\downarrow\uparrow\rangle - \uparrow\downarrow\uparrow\uparrow\rangle - \downarrow\uparrow\uparrow\uparrow\rangle\}$
-	1	0	$ \psi_{11}\rangle = \frac{1}{\sqrt{2}}\{ \uparrow\downarrow\uparrow\downarrow\rangle - \downarrow\uparrow\uparrow\downarrow\rangle\}, \psi_{12}\rangle = \frac{1}{\sqrt{2}}\{ \uparrow\uparrow\downarrow\downarrow\rangle - \downarrow\uparrow\downarrow\downarrow\rangle\}$
+	0	0	$ \psi_{15}\rangle = \frac{1}{2}\{ \uparrow\uparrow\downarrow\downarrow\rangle - \uparrow\downarrow\uparrow\downarrow\rangle - \uparrow\downarrow\downarrow\uparrow\rangle + \downarrow\uparrow\uparrow\downarrow\rangle\}, \psi_{16}\rangle = \frac{1}{\sqrt{12}}\{ \uparrow\uparrow\downarrow\downarrow\rangle + \uparrow\downarrow\uparrow\downarrow\rangle - 2 \uparrow\downarrow\downarrow\uparrow\rangle - 2 \downarrow\uparrow\uparrow\downarrow\rangle + \downarrow\uparrow\downarrow\uparrow\rangle + \downarrow\downarrow\uparrow\uparrow\rangle\}$

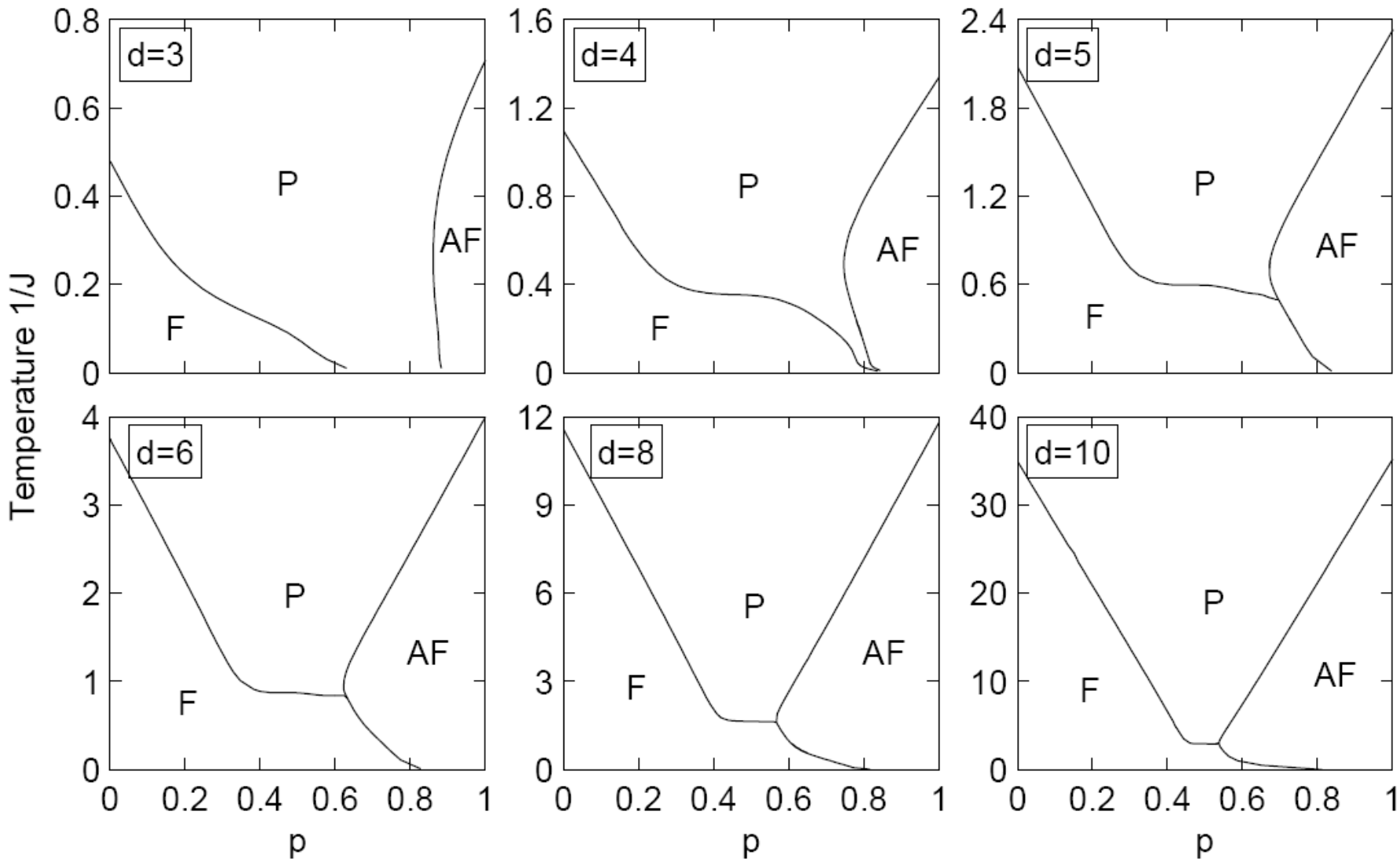
Klasik sistem (Ising) faz diyagramı

Migliorini ve ANB (1998)



Kuantum (Heisenberg) Sistemi Faz Diyagramları

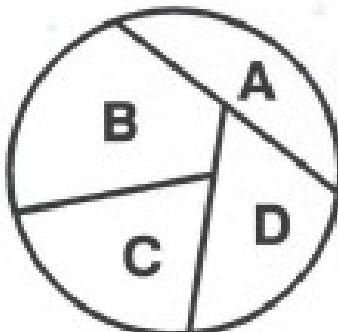
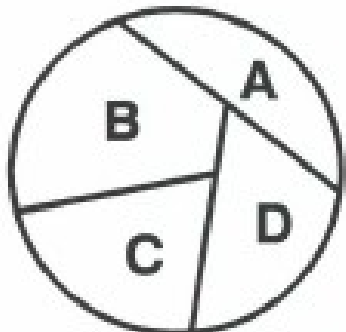
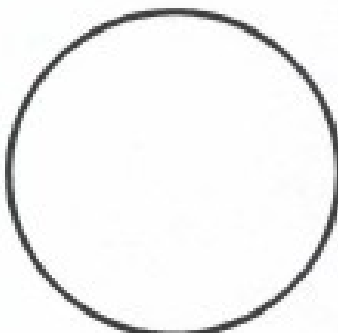
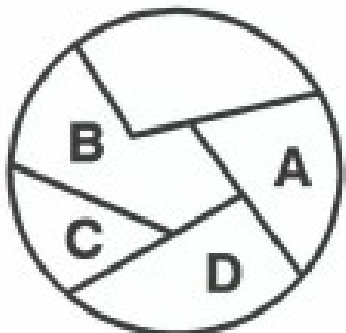
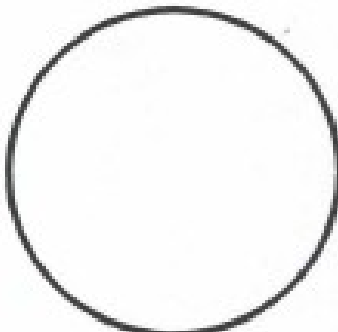
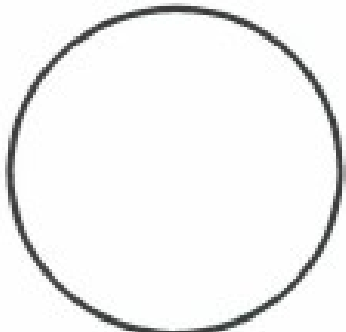
C.N. Kaplan ve ANB, Phys. Rev. Lett. [100](#), 027204 (2008)



IV. Quenched Bond Randomness Induced Criticality and the Strong Violation of Universality

Temperature

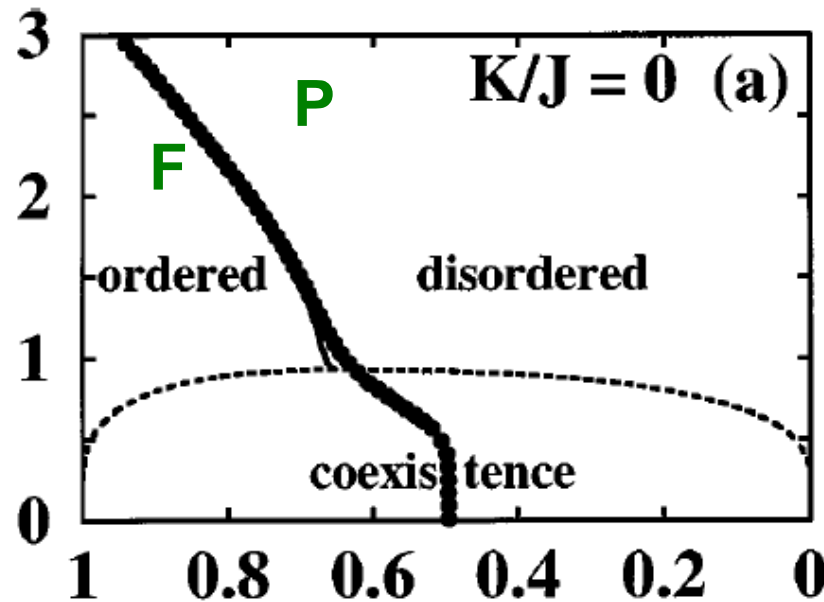
No random bonds With random bonds



With random bonds
(\equiv random temperature)
domain boundary
versus domain bulk free energy:
 L^{d-1} vs. $L^{d/2}$
1st order \rightarrow 2nd order
for infinitesimal randomness in $d=2$,
for finite randomness in $d=3$.
K. Hui and ANB, 1989

Temperature $1/J$

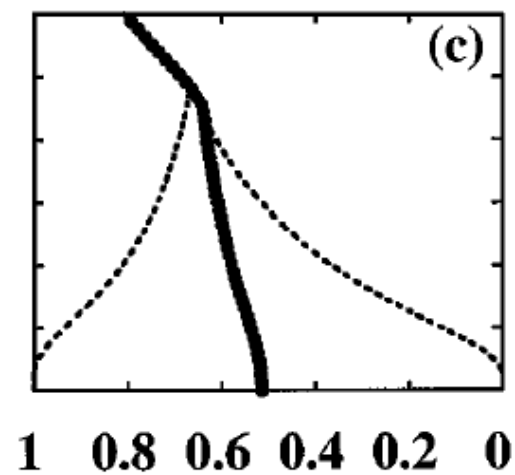
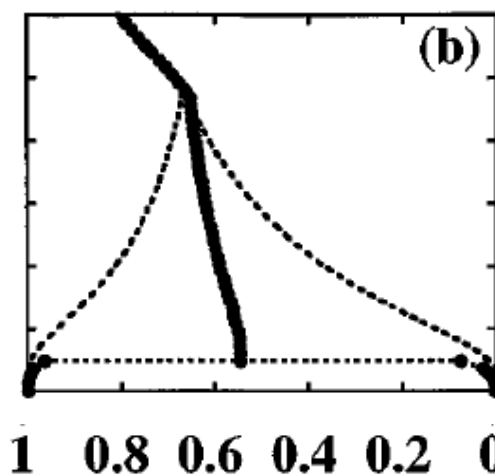
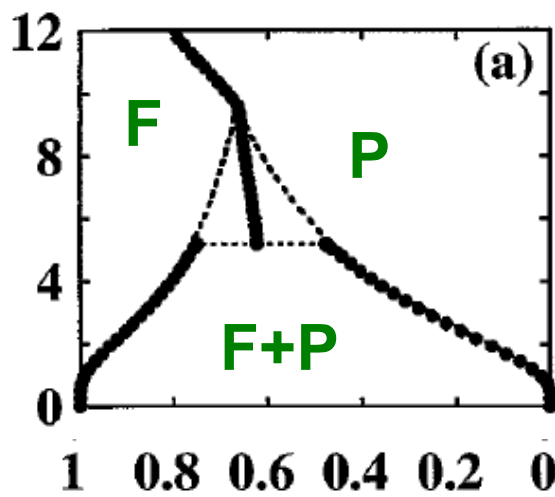
$d=2$

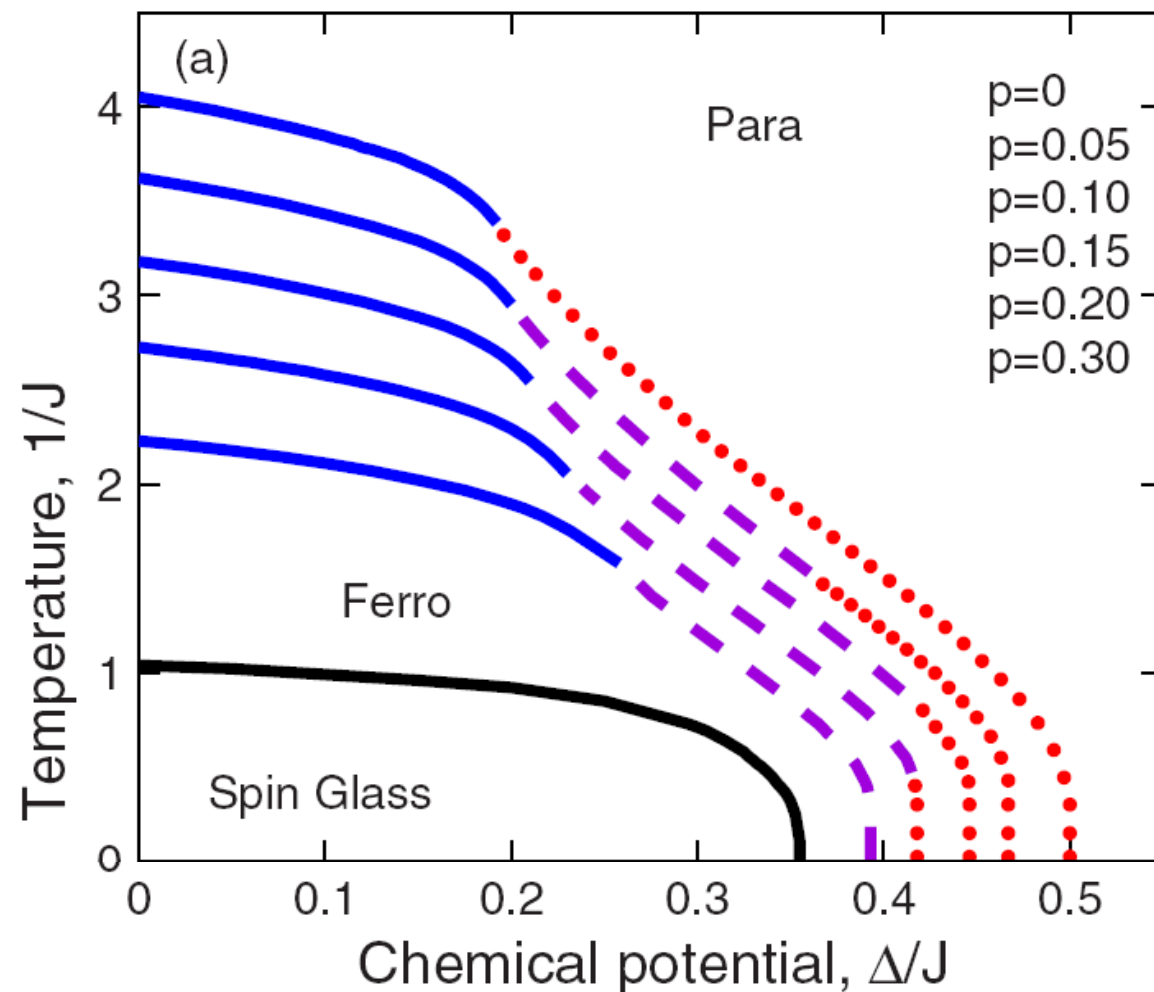


Random-bond
BEG model
 $s_i = \pm 1, 0$

$d=3$

Density $\langle s_i^2 \rangle$





Strong Violation of Critical Phenomena Universality: Wang-Landau Study of the 2d Blume-Capel Model under Bond Randomness

A. Malakis¹, A. Nihat Berker^{2,3,4}, I. A. Hadjiagapiou¹, and N. G. Fytas¹

¹*Department of Physics, Section of Solid State Physics,*

University of Athens, Panepistimiopolis, GR 15784 Zografos, Athens, Greece

²*College of Sciences and Arts, Koç University, Sarıyer 34450, Istanbul, Turkey*

³*Department of Physics, Massachusetts Institute of Technology, Cambridge, Massachusetts 02139, U.S.A.* and

⁴*Feza Gürsey Research Institute, TÜBİTAK - Bosphorus University, Çengelköy 34684, Istanbul, Turkey*

(Dated: September 24, 2008)

We study the pure and random-bond versions of the square lattice ferromagnetic Blume-Capel model, in both the first-order and second-order phase transition regimes of the pure model. Phase transition temperatures, thermal and magnetic critical exponents are determined for lattice sizes in the range $L = 20 - 100$ via a sophisticated two-stage numerical strategy of entropic sampling in dominant energy subspaces, using mainly the Wang-Landau algorithm. The second-order phase transition, emerging under random bonds from the second-order regime of the pure model, has the same values of critical exponents as the 2d Ising universality class, with the effect of the bond disorder on the specific heat being well described by double-logarithmic corrections, our findings thus supporting the marginal irrelevance of quenched bond randomness. On the other hand, the second-order transition, emerging under bond randomness from the first-order regime of the pure model, has a distinctive universality class with $\nu = 1.30(6)$ and $\beta/\nu = 0.128(5)$. These results amount to a strong violation of universality principle of critical phenomena, since these two second-order transitions, with different sets of critical exponents, are between the same ferromagnetic and paramagnetic phases. Furthermore, the latter of these two sets of results supports an extensive but weak universality, since it has the same magnetic critical exponent (but a different thermal critical exponent) as a wide variety of two-dimensional systems with and without quenched disorder. In the conversion by bond randomness of the first-order transition of the pure system to second order, we detect, by introducing and evaluating connectivity spin densities, a microsegregation that also explains the increase we find in the phase transition temperature under bond randomness.

Phys.Rev. E 79, 011125 (2009).

$\nu = 1$, double-log corrections; $\beta / \nu = \nu = 1.30(6)$; $\beta / \nu = 0.128(5)$

Strong
Violation of
Universality
Principle

Temperature $1/J$

3
2
1
0

1 0.8 0.6 0.4 0.2 0

Density $\langle s_i^2 \rangle$

$K/J = 0$ (a)

$d=2$

P

F
ordered

disordered

coexistence

Weak
Universality

Monte Carlo results
Malakis et al. 2009

(Pure Ising: $\nu = 1$; $\beta / \nu = 0.125$)

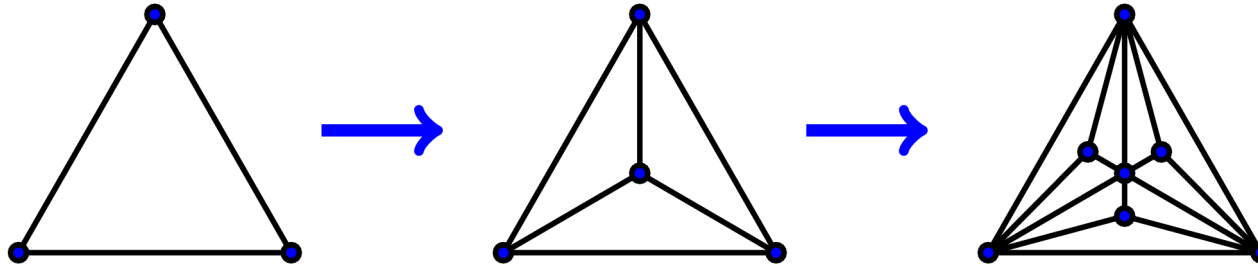
**V. Infinitely Robust Order and
Local Order-Parameter Tulips
in Apollonian Networks with Quenched Disorder**

C.N. Kaplan, M. Hinczewski, and ANB, arXiv:0811.3437v1 (2008).

Apollonian Networks with Quenched Disorder

C.N. Kaplan, M. Hinczewski, and A.N. Berker, arXiv:0811.3437

Construction of the network:



Since their introduction by J.S. Andrade Jr. *et. al.* [PRL 94, 018702 (2005)], **Apollonian* networks** have found a wide range of uses as a simple model incorporating three key features of real-world complex networks: a **scale-free degree distribution**, the **small-world effect**, and a **high clustering coefficient**.

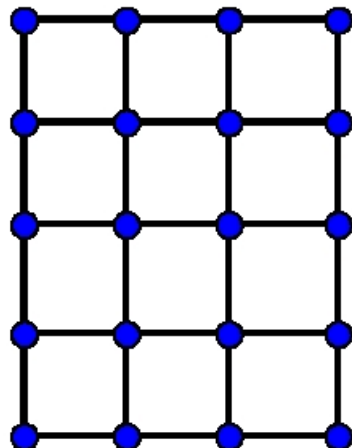
Spin systems on such networks are potentially physically realizable, for example in nanostructures formed from dense polydisperse packings of magnetic grains.

*Apollonius, Tangencies (Perge, Turkey, 3rd century BC)

Introduction: Properties of Complex Networks

We can illustrate various distinctive properties of real-world complex networks through a comparison to a regular lattice:

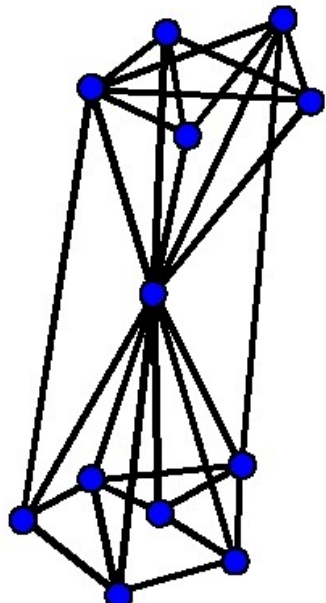
A ***d*-dimensional hypercubic lattice** has the properties:



- All sites have same degree (coordination number)
- The shortest-path distance between two sites, averaged over all pairs of sites in the lattice, scales like a power-law in the number of sites, $l \sim N^{1/d}$
- The lattice is unclustered: nearest-neighbors of a site are not nearest-neighbors of each other
- Critical behavior of simple spin systems like the Ising model described by power-law scaling of thermodynamic quantities near T_c

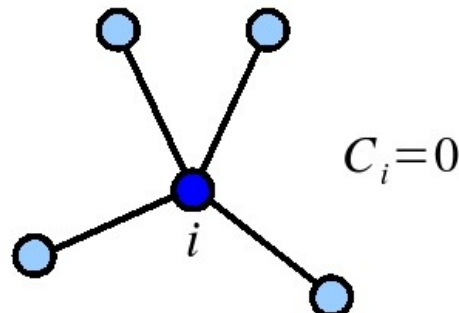
Introduction: Properties of Complex Networks

Many **real-world complex networks**, on the other hand, have one or more of the following characteristics:



- The degree k of a site is distributed with a probability $P(k)$ that is **scale-free**: for large k it decays like a power-law, $P(k) \sim k^{-\alpha}$
- The presence of long-distance bonds between sites leads to the **small-world effect**: logarithmic scaling in the average shortest-path length, $l \sim \log N$
- The network is **highly clustered**: nearest-neighbors of a site tend to be nearest-neighbors of each other
- Critical behavior varies with the details of the network: active field of research

Network Characteristics: Clustering Coefficient



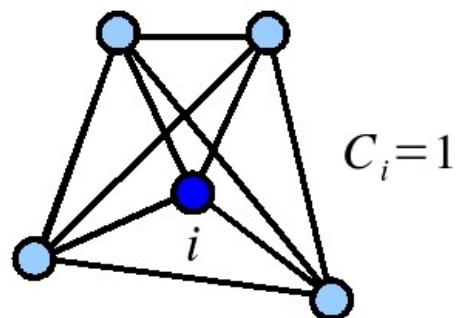
The clustering coefficient of a site i is:

$$C_i = \frac{B_i}{k_i(k_i-1)/2}$$

where

B_i = number of bonds among the n.n. of site i

k_i = degree of site i



For the network, the clustering coefficient is defined as:

$$C = \frac{1}{N} \sum_{\text{sites } i} C_i$$

Network Characteristics

Cumulative degree distribution, $P_{\text{cum}}(k) = \sum_{k'=k}^{\infty} P(k) \sim k^{1-\gamma}$
 $\gamma = 1 + \ln 3 / \ln 2 \approx 2.585$

Average shortest-path length, $\bar{l} \sim \ln N$

Average clustering coefficient, $C \approx 0.828$

- J.S. Andrade Jr., H.J. Herrmann, R.F.S. Andrade, and L.R. da Silva, Phys. Rev. Lett. **94**, 018702 (2005).
- J.P.K. Doye and C.P. Massen, Phys. Rev. E **71**, 016128 (2005).
- Z. Zhang, L. Chen, S. Zhou, L. Fang, J. Guan, and T. Zou, Phys. Rev. E **77**, 017102 (2008).

$$-\beta\mathcal{H} = \sum_{\langle ij \rangle} J_{ij} s_i s_j, \text{ where } s_i = \pm 1$$

Ferromagnetic ($J > 0$) and Antiferromagnetic ($J < 0$) Percolation

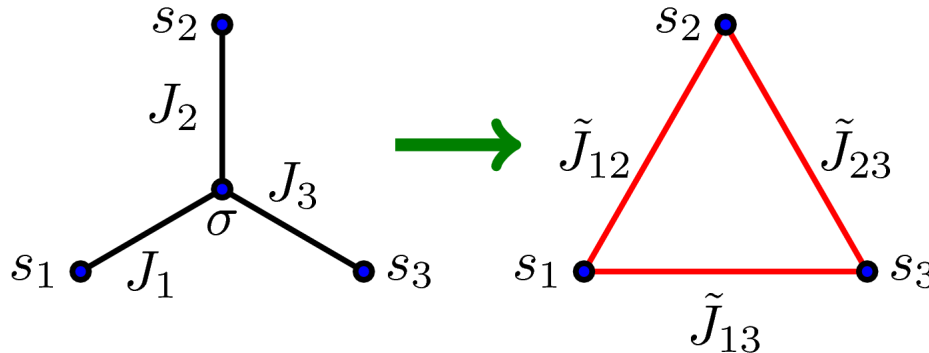
$$P(J_{ij}) = p\delta(J_{ij} - J) + (1 - p)\delta(J_{ij})$$

Spin Glass

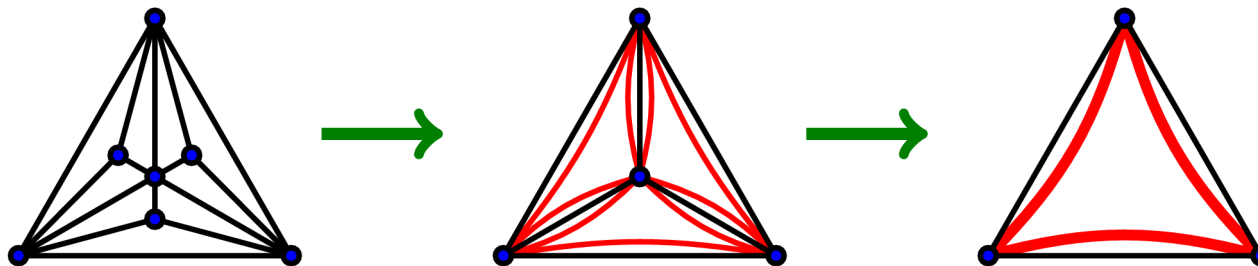
$$P(J_{ij}) = p\delta(J_{ij} + J) + (1 - p)\delta(J_{ij} - J)$$

RG for an Ising Model on the Apollonian Network

Star-triangle transformation:



This transformation can be carried out over all the plaquettes in the network:



The exact numerical RG procedure keeps track of the distribution of interactions in the renormalized triangles at each iteration.

Quenched Disorder: Nobre Method, with a pool of 10^6 interaction triplets

Results for Quenched-Random Ising Models

We investigated a variety of quenched-random Ising systems:

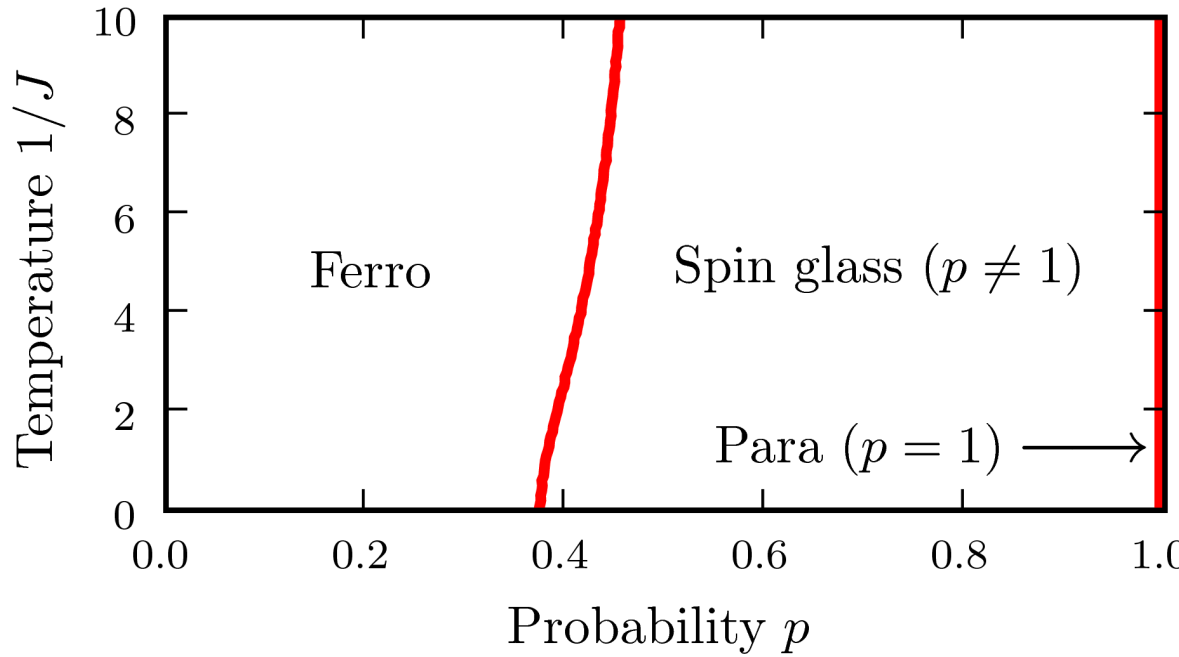
- Ferromagnetic / antiferromagnetic percolation system

Infinitely robust (all T) order: Ferro ($0 < p$) / Spin Glass ($0 < p < 1$)

- Spin-glass system

In all cases we find **infinitely robust order** — ordered phases persist up to infinite temperature for any amount of imposed quenched disorder.

Spin-glass phase diagram as a function of the AF bond probability:



Red lines
mark first-order
phase transitions.

Long-range
interactions

Calculation of Local Magnetizations: by summation along RG trajectories

$$m_\sigma = \boldsymbol{\mu}^{(i)T} T^{(i)} T^{(i-1)} \dots T^{(2)} \mathbf{V}^{(1)},$$
$$\mu_\alpha^{(i)} = \partial \ln Z / \partial K_\alpha^{(i)},$$

$$T_{\beta\alpha}^{(i)} = \partial K_\beta^{(i)} / \partial K_\alpha^{(i-1)}, V_\alpha^{(1)} = \partial K_\alpha^{(1)} / \partial H_\sigma,$$
$$\mathbf{K}^{(i)} \equiv \{H_1^{(i)}, H_2^{(i)}, H_3^{(i)}, K^{(i)}\}$$



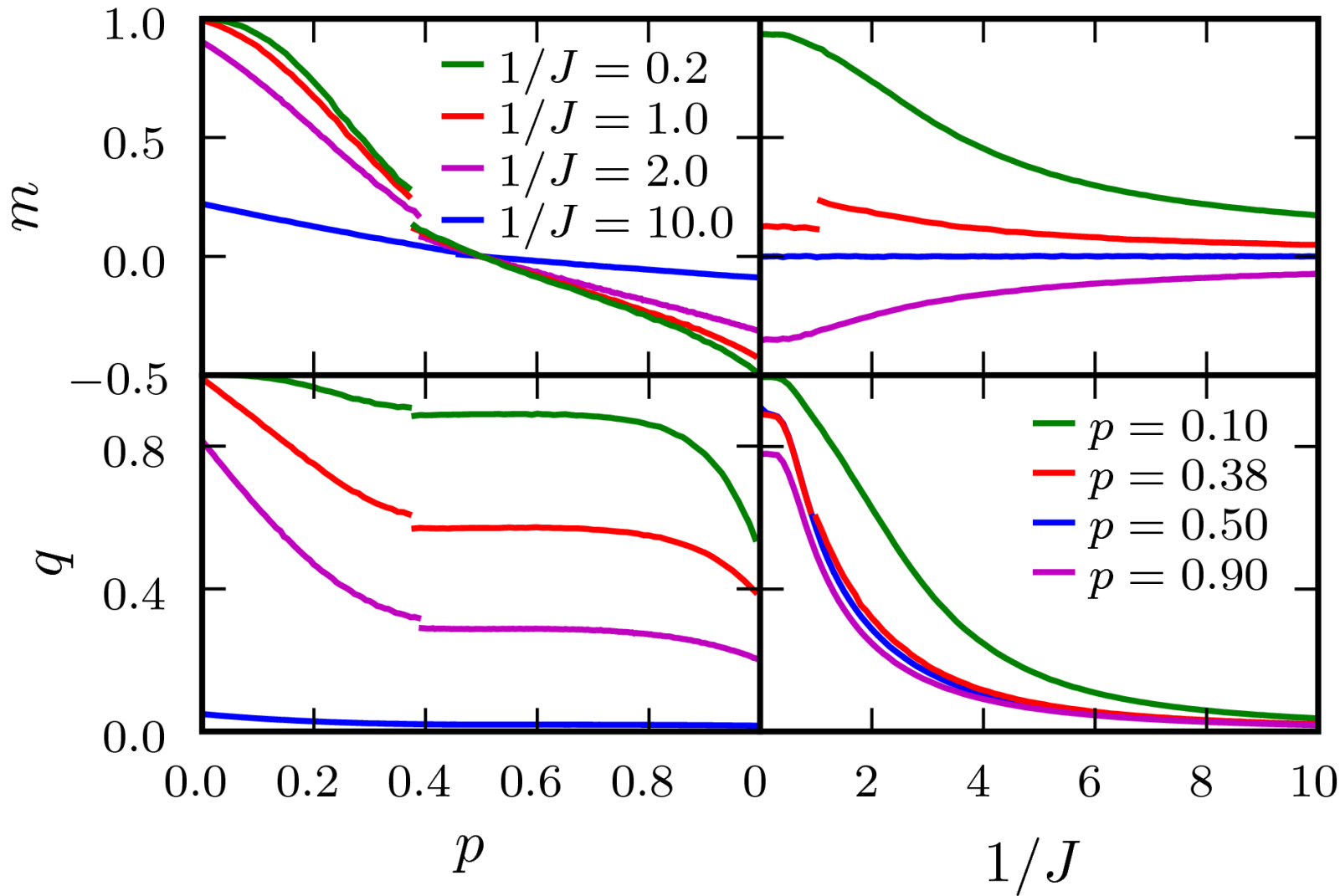
T=0.5

Low-temperature d=2 spin-glass local energies
D. Yeşiltepen and ANB, 1997



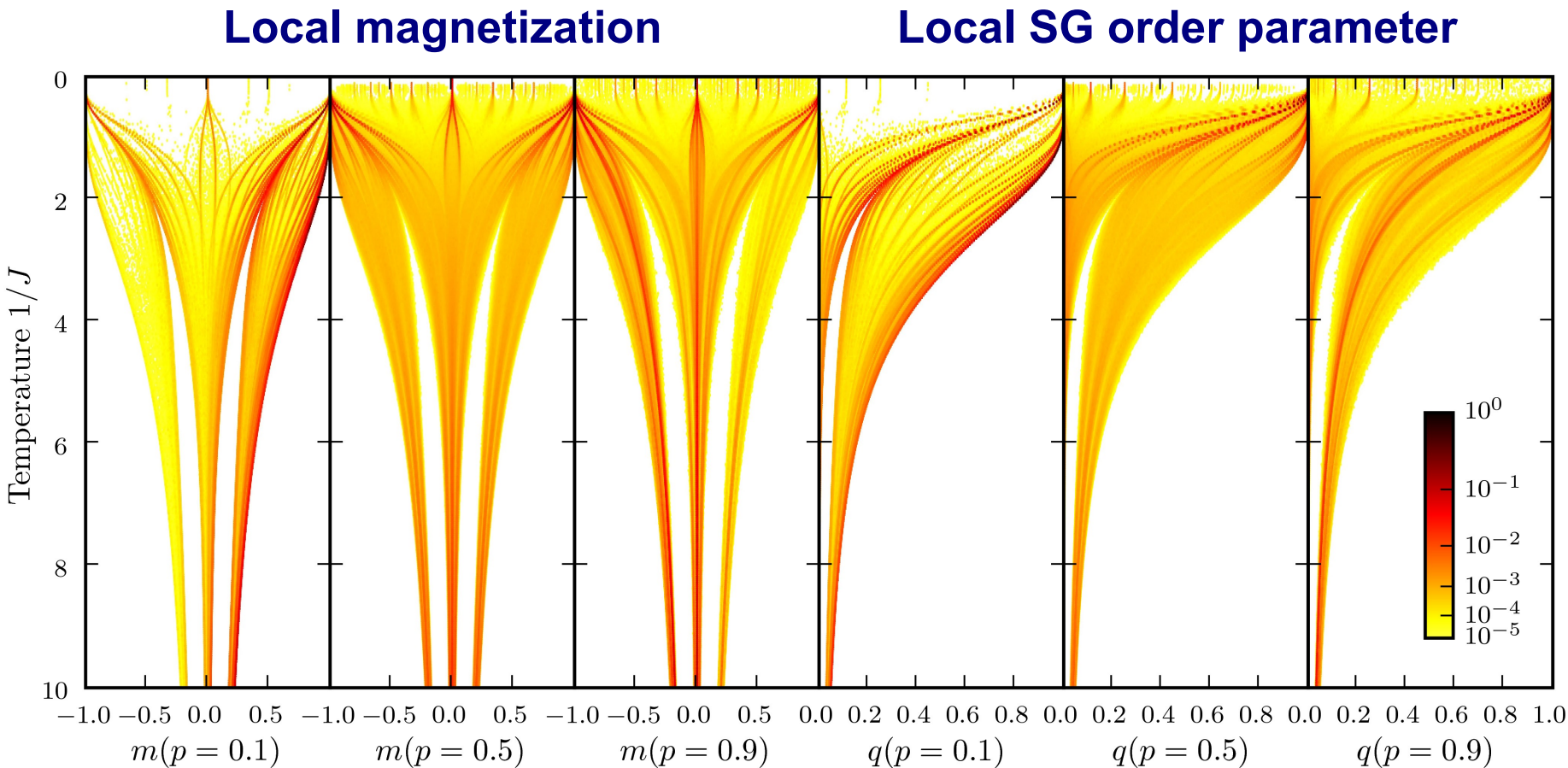
Average Order Parameters for Ising Spin Glass

$$m_i = \langle s_i \rangle, \quad m = \frac{1}{N} \sum_i m_i, \quad q = \frac{1}{N} \sum_i m_i^2$$



Local Order Parameter “Tulips”

Exact numerical distributions for the local magnetization and spin-glass order parameters show complex tulip-like patterns as a function of temperature:









Nadir Kaplan

Return trip from 100. Stat Mech Conf
Rutgers U, December 2008

Ongun Özçelik



Sabancı University, Istanbul

